Interactions of *cis*-P_2PtX_2 Complexes (X = H, CH_3) with Bis(pentamethylcyclopentadienyl)ytterbium

David J. Schwartz, Graham E. Ball, and Richard A. Andersen*

Contribution from the Chemistry Department and Chemical Sciences Division of Lawrence Berkeley Laboratory, University of California, Berkeley, California 94720

Received December 6, 1994[⊗]

Abstract: The interactions formed in solution between the bent lanthanide metallocene Cp^*_2Yb (**1**) and *cis*-P_2PtX_2 complexes (P_2 = a chelating phosphine; X = H, CH_3) have been investigated using NMR spectroscopy. **1** has been found to form a significant interaction with the *cis* dihydride complexes $[(Cy)_2P(CH_2)_nP(Cy)_2]PtH_2$ (n = 2, dcype, **4**; n = 3, dcypp, **6**). Intermolecular exchange is slow on the NMR time scale for a 1:1 sample of **1** and **4**, and there are significant perturbations in the spectral values from those of free **4**. Additionally, $^1J_{YbH}$ of 180 Hz and J_{PtYb} of 2260 Hz are present. A sample of **1** and **6** gives almost identical spectral values. Fast intermolecular exchange (NMR) occurs for samples containing an excess of the dihydride complexes but not for samples containing an excess of **1**. The NMR values of a 1:1 sample of the dimethyl complex (dippe)$Pt(CH_3)_2$ (dippe = $(^iPr)_2P(CH_2)_2P(^iPr)_2$) (**8**) and **1** are perturbed from the analogous values for free **8**, but fast intermolecular exchange is present on the NMR time scale down to −90 °C. The solid-state structure of this adduct, **9**, shows a rare mode of an agostic bridging methyl interaction; however, $^1J_{CH_3}$ is unchanged from that of **8**. Crystal data for **9**: monoclinic, space group $C2/c$, with a = 33.90(2) Å, b = 11.255(6) Å, c = 20.535(6) Å, β = 98.41(4)°, V = 7750(7) Å^3, Z = 8, final R = 0.029 for 361 variables, and 3300 data with $I > 3\sigma(I)$. A 1:1 sample of **1** and a methyl hydride complex, (dippe)$Pt(CH_3)$-(H) (**10**) undergoes slow exchange in solution, with $^1J_{YbH}$ of 168 Hz and J_{PtYb} of 960 Hz. Again $^1J_{CH_3}$ is unchanged from that of free **10**. The Yb−CH_3 interaction likely arises from geometrical constraints, the Yb−hydride interaction holding the Yb center near the methyl group. The solid-state structure of this adduct, **11**, shows an asymmetric (μ-CH_3)(μ-H) bridge. Crystal data for **11**: monoclinic, space group $P2_1/c$, with a = 18.778(5) Å, b = 10.903(4) Å, c = 20.255(5) Å, β = 114.74(2)°, V = 3766 (2) Å^3, Z = 4, final R = 0.069 for 327 variables, and 4694 data with $I > 3\sigma(I)$. The NMR perturbations and coupling constants resulting from the interactions of **1** with the P_2PtX_2 complexes are discussed in detail and correlated with the solid-state structures. The ^{195}Pt and ^{171}Yb chemical shifts of **1**, the Pt(II) complexes, and the 1:1 adducts are also reported.

Introduction

The metallocene Cp^*_2Yb has a bent sandwich strucutre in the gas phase, with a centroid−Yb−centroid angle of 158° in the thermal average structure.[1] One consequence of this bent geometry is that the enthalpy of adduct formation does not have to compensate for the reorganization energy of bending, making Cp^*_2Yb an excellent candidate for examining weak metal−ligand bonding. This closed-shell ($4f^{14}$ electron configuration) Lewis acid can be used to study the solid-state geometrical changes that occur upon adduct formation, and this has been informative, particularly when coordination complexes are formed with ligands that are not generally viewed as good ligands for f-block metals. For example dimethylacetylene forms an adduct with Cp^*_2Yb in which the acetylene is η^2-bound, with bond distances and angles that are essentially unchanged relative to those of the free ligand.[2a] A similar result is apparent in the solid-state structure of $[(CH_3)_4EtC_5]_2YbC[N(CH_3)C(CH_3)=C(CH_3)N(CH_3)]$.[2b] In the unusual adduct with $Cp^*Be(CH_3)$, the $Be(CH_3)$ moiety coordinates to Cp^*_2Yb in a linear Yb−C−Be fashion, such that there are short Yb- -H distances.[2c] Similar interactions, with short Yb- -H distances, are found in the solid-state structure of $Cp^*_2Yb(\mu\text{-}C_2H_4)Pt(PPh_3)_2$,[2d] though the other structural features are essentially unchanged relative to the uncomplexed fragments. Since the solid-state geometrical changes are small in these adducts, it is not surprising that in solution there is a small barrier to dissociation into their individual fragments; these complexes exhibit rapid intermolecular exchange on the NMR time scale at all temperatures. As a consequence, only average spectroscopic values for these and related molecules[3] are known.

Bis(pentamethylcyclopentadienyl)ytterbium is potentially an ideal Lewis acid for exploring the kinetics and thermodynamics of weak metal−ligand bonding by NMR spectroscopy, if compounds can be prepared for which intermolecular exchange is slow on the NMR time scale. This is due to the facts that the coordination complexes are diamagnetic and ^{171}Yb (14.3% natural abundance) has a nuclear spin of $^1/_2$. The presence or absence of spin−spin coupling can be used to judge whether chemical exchange is occurring.[4] The perturbations in the NMR

* Address correspondence to this author at Chemistry Department, University of California, Berkeley, CA 94720.

⊗ Abstract published in *Advance ACS Abstracts,* May 15, 1995.

(1) (a) Andersen, R. A.; Boncella, J. M.; Burns, C. J.; Green, J. C.; Hohl, D.; Rosch, N. *J. Chem. Soc., Chem. Commun.* **1986**, 405. (b) Andersen, R. A.; Boncella, J. M.; Burns, C. J.; Blom, R.; Haaland, A.; Volden, H. V. *J. Organomet. Chem.* **1986**, *312*, C49. (c) Andersen, R. A.; Blom, R.; Boncella, J. M.; Burns, C. J.; Volden, H. V. *Acta Chem. Scand.* **1987**, *A41*, 24. (d) Green, J. C.; Hohl, D.; Rosch, N. *Organometallics* **1987**, *6*, 712.

(2) (a) Burns, C. J.; Andersen, R. A. *J. Am. Chem. Soc.* **1987**, *109*, 941. (b) Schumann, H.; Glanz, M.; Winterfeld, J.; Hemling, H.; Kuhn, N.; Kratz, T. *Angew. Chem., Int. Ed. Engl.* **1994**, *33*, 1733. (c) Burns, C. J.; Andersen, R. A. *J. Am. Chem. Soc.* **1987**, *109*, 5853. (d) Burns, C. J.; Andersen, R. A. *J. Am. Chem. Soc.* **1987**, *109*, 915.

(3) (a) Tilley, T. D.; Andersen, R. A.; Spencer, B.; Ruben, H.; Zalkin, A.; Templeton, D. H. *Inorg. Chem.* **1980**, *19*, 2999. (b) Tilley, T. D.; Andersen, R. A.; Spencer, B.; Zalkin, A. *Inorg. Chem.* **1982**, *21*, 2647. (c) Tilley, T. D.; Andersen, R. A.; Zalkin, A. *Organometallics* **1983**, *2*, 856.

(4) (a) Kidd, R. G.; Goodfellow, R. J. In *NMR and the Periodic Table;* Harris, R. K., Mann, B. E., Eds.; Academic Press Inc.: New York, 1978. (b) Avent, A.; Edelman, M. A.; Lappert, M. F.; Lawless, G. A. *J. Am. Chem. Soc.* **1989**, *111*, 3423.

0002-7863/95/1517-6027$09.00/0

spectral values as well as the presence and size of coupling to ^{171}Yb can give information concerning the nature of the interactions in solution. The other readily available bivalent lanthanide metallocenes, Cp^*_2Sm and Cp^*_2Eu, do not have NMR-active nuclei with $I = {}^1/_2$, and they are paramagnetic.[5] The paramagnetic shift induced by Cp^*_2Eu has been used to study weak metal−ligand bonding in an indirect way.[6] The recent report that spin−spin coupling was observed between ytterbium and hydrogen in d-transition metal hydride anions[7] indicates that the hydride ligand might be a candidate for stopping intermolecular chemical exchange. In this manuscript, we describe the solution- and solid-state perturbations resulting from the Lewis acid−base interactions between Cp^*_2Yb and *cis*-P_2PtX_2 complexes, where X = H and CH_3.

Results

Interaction with *cis*-$[R_2P(CH_2)_2PR_2]PtH_2$. Addition of a colorless toluene solution of *cis*-$[(Me_3C)_2PCH_2CH_2P(CMe_3)_2]PtH_2$, (dtbpe)$PtH_2$ (**2**),[8] to a brown toluene solution of Cp^*_2Yb (**1**) at room temperature results in the immediate precipitation of a maroon solid, formulated as (dtbpe)Pt(μ-H)$_2$YbCp^*_2 (**3**), in quantitative yield. The solid-state infrared spectrum of this complex shows ν(M−H) bands at 1925 and 1898 cm^{-1}, shifted from the single broad absorption of 1988 cm^{-1} for **2**. While this shift to lower energy is characteristic of bridging Pt hydride ligands, it is a smaller perturbation then is generally observed,[9] indicating that the Yb−hydride interactions are relatively weak. The adduct is completely insoluble in hexane, toluene, and diethyl ether. Although it dissolves in tetrahydrofuran-d_8 to give a maroon solution, the ^{1}H and ^{31}P NMR data show that the solution contains free **2** and the known $Cp^*_2Yb(thf)_2$ adduct.[10] Integration of the proton NMR spectrum of this sample shows that **3** is indeed a 1:1 adduct. The solubility properties of **3** precluded further study of this complex.

Allowing **1** to react with 1 equiv of *cis*-$[(Cy)_2PCH_2CH_2P(Cy)_2]PtH_2$, (dcype)$PtH_2$ (**4**), in toluene gives a dark blue solution. Slow cooling of this solution to −80 °C gives dark maroon crystals of the 1:1 complex (dcype)Pt(μ-H)$_2$YbCp^*_2 (**5**), in 75% yield. This complex shows a broad band at 1889 cm^{-1} in its solid-state infrared spectrum, shifted to lower energy relative to the ν(M−H) bands for **4**, at 1986 and 1979 cm^{-1}. Crystals of **5**, isolated from toluene, do not redissolve in toluene. Consequently, the NMR data discussed below were obtained on a sample that was made by dissolving **4** and a slight excess of **1** in C_6D_6. This sample will hereafter be referred to either as the 1:1 sample or simply as the complex **5**.

The ^{1}H and ^{31}P{^{1}H} NMR spectra of **4** and the 1:1 sample, at 25 °C, are shown in Figure 1. In addition to the expected spin−spin coupling of the hydride nuclei to the two phosphorus nuclei and to the ^{195}Pt isotope ($I = {}^1/_2$, 33.8% natural abundance), coupling to ^{171}Yb is also present in the ^{1}H NMR spectrum of **5** (Figure 1b, $^1J_{YbH}$ = 180 Hz). Coupling of the phosphorus nuclei to ^{171}Yb is also present (Figure 1d, J_{YbP} = 93 Hz), the intensity of each satellite being *ca.* 7% of the intensity of the major resonance, as expected. The presence of these couplings indicates that intermolecular exchange is slow on the NMR time scale, at 25 °C.

Interestingly, while intermolecular exchange does not occur at 25 °C for a sample of **1** and **4** containing a slight excess of **1**, this is not true for a sample containing an excess of **4**. Fast intermolecular exchange is observed at 25 °C on the NMR time scale, when **1** and **4** are mixed in a 1:2 molar ratio. The spectra show broadened resonances, coupling to ^{171}Yb is no longer observed, and the chemical shift and coupling constant values are averages of the stopped exchange values and the values for free **1** and **4**. One possible rationalization of this result is that an associative exchange mechanism occurs when **4** is present in excess, the transition state involving interaction of an Yb center with one hydride ligand on each of two different molecules of **4**, as shown in Figure 2. If the exchange mechanism were dissociative, the presence of excess **4** would have a negligible effect on the exchange rate; also, for a dissociative mechanism, the presence of excess **1** would be expected to result in fast exchange. Presumably, the steric bulk of the Cp* rings prevents two molecules of **1** from simultaneously coordinating to one molecule of **4** (Figure 2), resulting in a higher barrier and therefore slow exchange behavior for a sample containing excess **1**.

In contrast to **3**, dissolution of **5** in tetrahydrofuran-d_8 does not result in complete cleavage of the 1:1 complex formed from **1** and **4**. Rather, values intermediate between the stopped-exchange values of the 1:1 sample (in C_6D_6) and the values of free **4** in tetrahydrofuran-d_8 are observed, along with broadened resonances and loss of coupling to ^{171}Yb, at 25 °C. Qualitatively, this indicates that **4** and thf are comparable Lewis bases, relative to the Lewis acid $YbCp^*_2$ (keeping in mind that thf is present in large excess in this sample). The apparent relative basicity series is thf ≈ (dcype)PtH_2 (**4**) > (dtbpe)PtH_2 (**2**). This difference between **2** and **4** may be the result of steric effects. The dcype derivative possesses a proton on the α carbon of the cyclohexyl ring, while the dtbpe derivative has only methyl groups on this carbon; this may result in destabilizing steric interactions between **1** and **2**, as compared to the steric interactions formed between **1** and **4**. Such differences in steric effects for dcype *vs* dtbpe complexes have been reported.[11]

The ^{1}H/^{195}Pt and ^{1}H/^{171}Yb correlation 2-D spectra obtained on **5** at 25 °C are shown in Figures 3 and 4, respectively. These spectra, and most of the other spectra obtained to measure metal chemical shifts and coupling patterns in this work, were obtained using the 2D-HMQC pulse sequence,[12] which allows indirect detection of an X nucleus with ^{1}H sensitivity, utilizing a J_{XH} coupling. Couplings to ^{1}H are essentially removed in the X dimension. Equally important is the fact that couplings to a different type of nucleus, Y, in an H−X correlation are independently retained in both dimensions, resulting in an E.COSY-like splitting pattern,[13] with respect to the Y nucleus. Resolution of splittings into two dimensions allows easier identification of coupling constants found in lower intensity isotopomers (e.g., when Y = ^{171}Yb), particularly when satellites due to these isotopomers would be obscured by other lines in the relevant 1-D spectra. A large splitting due to coupling to Y in one dimension may be used to resolve a small coupling to Y in the other dimension, even if this small coupling is less

(5) (a) Berg, D. J.; Burns, C. J.; Andersen, R. A.; Zalkin, A. *Organometallics* **1989**, *8*, 1865. (b) Evans, W. J.; Hughes, L. A.; Hanusa, T. P. *Ibid.* **1986**, *5*, 1285.

(6) Nolan, S. P.; Marks, T. J. *J. Am. Chem. Soc.* **1989**, *111*, 8538.

(7) Green, M. L. H.; Hughes, A. K.; Michaelidou, D. M.; Mountford, P. *J. Chem. Soc., Chem. Commun.* **1993**, 591.

(8) Yoshida, T.; Yamagata, T.; Tulip, T. H.; Ibers, J. A.; Otsuka, S. *J. Am. Chem. Soc.* **1978**, *100*, 2063.

(9) (a) Green, M.; Howard, J. A. K.; Proud, J.; Spencer, J. L.; Stone, F. G. A.; Tsipis, C. A. *J. Chem. Soc., Chem. Commun.* **1976**, 671. (b) Ciriano, M.; Green, M.; Proud, J.; Spencer, J. L.; Stone, F. G. A.; Tsipis, C. A. *J. Chem. Soc., Dalton Trans.* **1978**, 801. (c) Tulip, T. H.; Yamagata, T.; Yoshida, T.; Wilson, R. D.; Ibers, J. A.; Otsuka, S. *Inorg. Chem.* **1979**, *18*, 2239.

(10) Watson, P. L. *J. Chem. Soc., Chem. Commun.* **1980**, 652.

(11) Schwartz, D. J.; Andersen, R. A. *J. Am. Chem. Soc.* **1995**, *117*, 4014.

(12) (a) Bax, A.; Griffey, R. H.; Hawkins, B. L. *J. Magn. Reson.* **1983**, *55*, 301. (b) Bax, A.; Subramanian, S. *J. Magn. Reson.* **1986**, *67*, 565.

(13) (a) Emerson, S. D.; Montelione, G. T. *J. Am. Chem. Soc.* **1992**, *114*, 354. (b) Griesenger, C.; Sorensen, O. W.; Ernst, R. R. *J. Am. Chem. Soc.* **1985**, *107*, 6394.

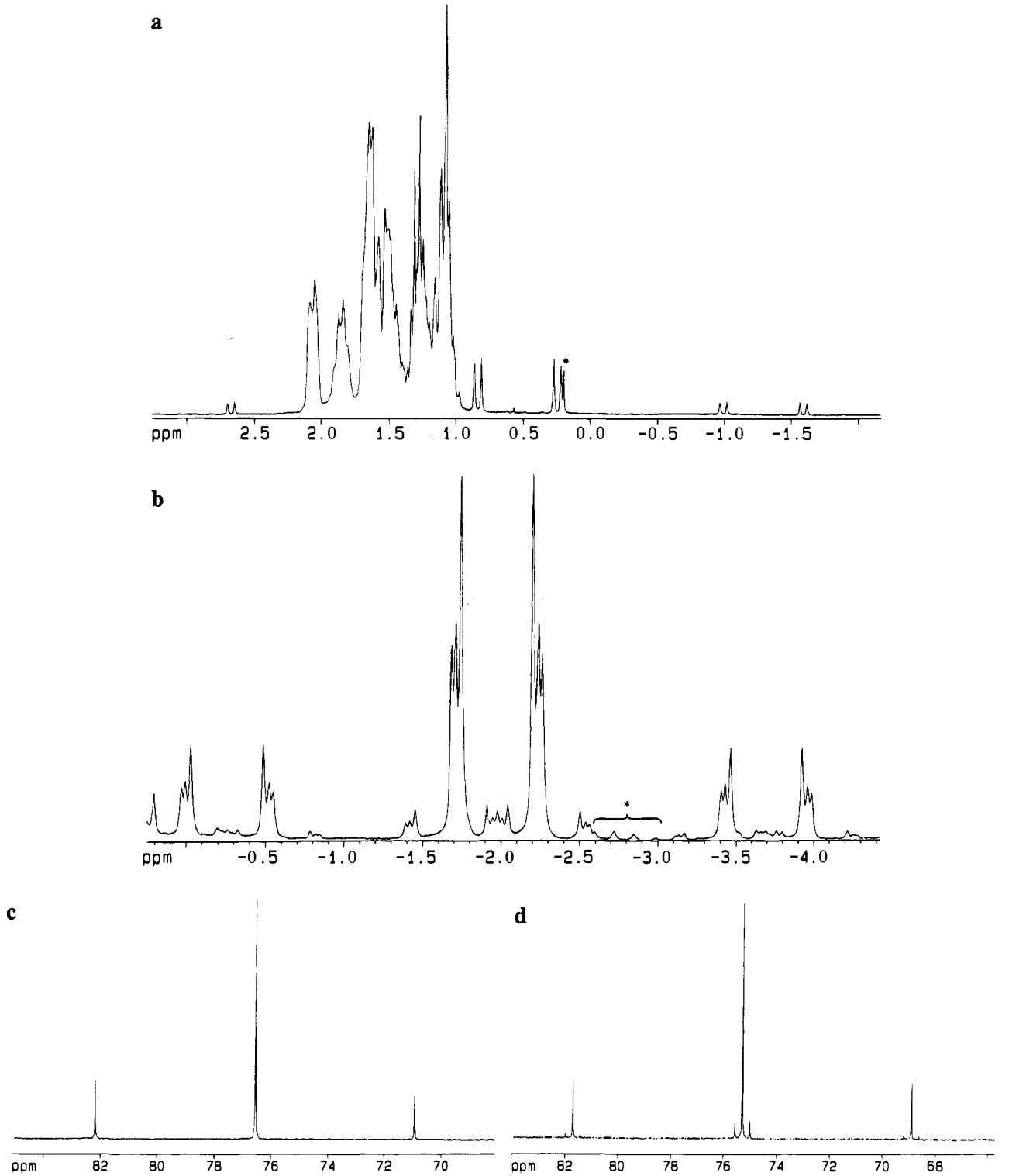

Figure 1. ^1H and $^{31}P\{^1H\}$ NMR spectra of **4** and **5** (C_6D_6, 25 °C); (a) ^1H spectrum of **4** (300 MHz; a minor grease impurity is marked with an asterisk), (b) ^1H spectrum of **5** (300 MHz; hydride region; a minor impurity is marked with an asterisk), (c) $^{31}P\{^1H\}$ spectrum of **4** (162 MHz), (d) $^{31}P\{^1H\}$ spectrum of **5** (162 MHz).

than the line width in that dimension. Information about the relative signs of coupling constants may also be directly inferred from the direction of the slope in the E.COSY-like pattern.

In the case of **5**, the $^1H/^{171}Yb$ HMQC spectrum confirms that ^{171}Yb is the source of the extra satellites present in the ^1H and $^{31}P\{^1H\}$ NMR spectra (Figure 1). In addition, the ^{195}Pt and ^{171}Yb pseudospectra (vertical dimensions in Figures 3 and 4, respectively) contain a triplet with ^{195}Pt satellites and a triplet with ^{171}Yb satellites, respectively (the triplets arise from coupling to the two phosphorus nuclei), showing that there is coupling between the metal centers. The $^1H/^{195}Pt$ spectrum (Figure 4) shows that this coupling, J_{PtYb}, has the same sign as $^1J_{PtH}$. The NMR spectral values measured on **5** are presented in Table 1, along with the values for **4**. Since the signs of $^1J_{PtH}$ and $^1J_{PtP}$ are known to be positive,[14] the signs of the other coupling constants can be obtained from the HMQC spectra and are shown in Table 1.

(14) Pregosin, P. S. In *Transition Metal Nuclear Magnetic Resonance*; Pregosin, P. S., Ed.; Elsevier Science Publishing Co. Inc.: New York, 1991; pp 234–242 and references therein.

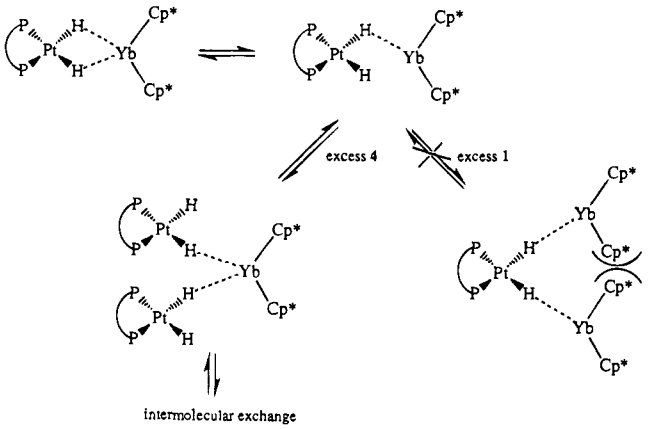

Figure 2. Proposed exchange mechanism for a sample containing **1** with an excess of **4**.

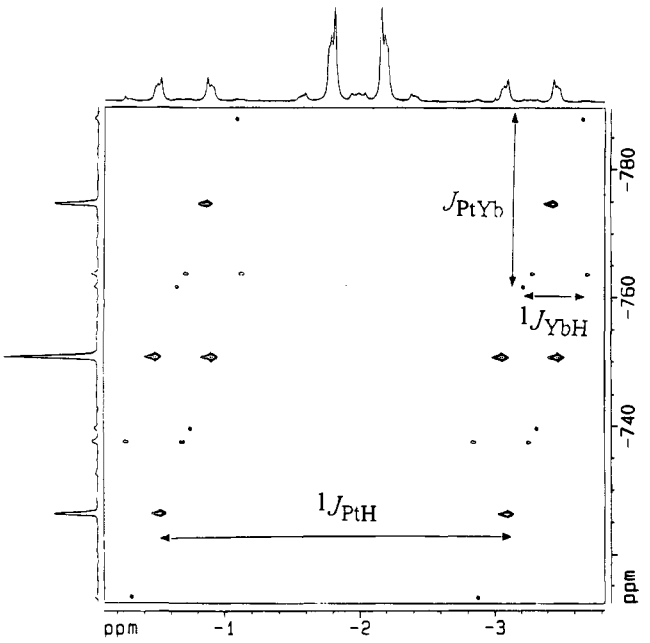

Figure 3. $^1H/^{195}Pt$ HMQC NMR spectrum of **5** (400 MHz, C_6D_6, 25 °C). Annotated with normal ^1H spectrum (F2) and ^{195}Pt projection (F1).

Interaction of **1** with **4** results in several perturbations in the chemical shift and coupling constant values, compared with the values for uncomplexed **4**. Specifically, a significant upfield shift of δ(Pt−*H*) by 2.54 ppm occurs, indicating that the bridging hydrides of **5** are more shielded, relative to those of **4**. The Cp* resonance of **1** is shifted downfield by 0.47 ppm; downfield shifts of this resonance are common for $Cp^*_2YbL_n$ complexes, relative to the value for **1**.[2a,d]

The interaction between **1** and **4** results in a decrease in the $^2J_{PH}$ and $^1J_{PtH}$ values and a large increase in the $^1J_{PtP}$ value. These perturbations are easily rationalized by assuming that donation of electron density from the Pt−hydride bonds to the acidic ytterbium metal center results in a decrease in the Pt−H bond strength and a consequent decrease in the *trans* influence of the hydride ligands. Bridging hydride ligands in dimeric Pt phosphine complexes generally have a lower *trans* influence then terminal Pt hydrides.[11,15] Consistent with the IR data for **5** (see above), the $^1J_{PtH}$ value for **5** (1031 Hz) is lowered from the value for free **4** but is still higher than is generally seen for bridging Pt hydrides,[16] indicating that the Yb−hydride interaction is relatively weak. Interaction of **1** with the H/D analogue of **4**, (dcype)Pt(H)(D), shows no sign of $^1J_{HD}$ in the ^1H NMR spectrum; the half-height width of the resonances is *ca.* 15 Hz, indicating that J_{HD} is less then *ca.* 8 Hz. The $^1J_{HD}$ value for free (dcype)Pt(H)(D), at 25 °C and at −80 °C, was found to be near zero.[17]

There have been few J_{YbH} and J_{YbP} values reported in the literature; the values measured on **5** are similar to the previously reported values. The $^1J_{YbH}$ value of 180 Hz found for **5** can be compared to the values of 170 Hz for $[\{CpNb(\mu\text{-}H)_2\}_2Yb(diglyme)]$[7] and 200 Hz for $[(Tp')Yb(\mu\text{-}HBEt_3)(thf)]$ (Tp′ = hydrotris(3-*tert*-butyl-5-methylpyrazolyl)borate).[18] The $^3J_{YbP}$ value of 93 Hz in **5** is similar to the value of 73 Hz found for

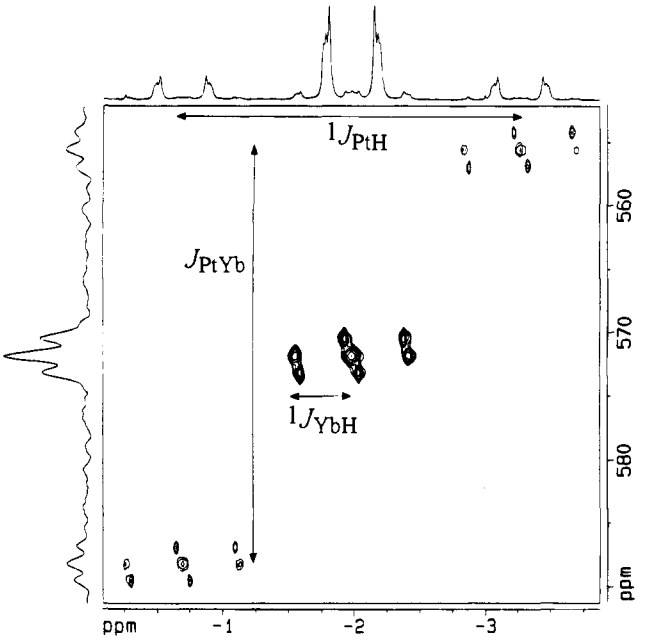

Figure 4. $^1H/^{171}Yb$ HMQC NMR spectrum of **5** (400 MHz, C_6D_6, 25 °C). Annotated with normal ^1H spectrum (F2) and ^{171}Yb projection (F1).

Table 1. ^1H, ^{31}P, ^{195}Pt, and ^{171}Yb NMR Data for **4** and **5** (C_6D_6, 25 °C)

	4	**5**
δ(Pt−*H*), ppm	0.56	-1.98
$^2J_{PH}$(*trans,cis*), Hz[a]	+179, −16	+152, −14
$^1J_{PtH}$, Hz	+1100	+1031
δ(P), ppm	76.5	75.4
$^1J_{PtP}$, Hz	+1822	+2077
δ(Cp*), ppm	*b*	2.42
$^1J_{YbH}$, Hz		+180
J_{YbP}, Hz		+93
δ(Pt), ppm[c]	−862	−751
δ(Yb), ppm[c]	−50[d]	+572
J_{YbPt}, Hz		+2260

[a] Unless otherwise stated, J_{XH} pertains to the coupling constant involving the nucleus X and the hydride nuclei in all of the tables. [b] The chemical shift for the Cp* protons for a C_6D_6 sample of **1** is 1.93 ppm. [c] For details of the metal chemical shift referencing, see the Experimental Section. [d] The ^{171}Yb chemical shift for **1**, measured at +60 °C using direct detection ($w_{1/2}$ = 100 Hz).

(15) Bracher, G.; Grove, D. M.; Pregosin, P. S.; Venanzi, L. M. *Angew. Chem., Int. Ed. Engl.* **1979**, *18* , 155.

(16) (a) Naegeli, R.; Togni, A.; Venanzi, L. M. *Organometallics* **1983**, *2*, 926. (b) Boron, P.; Musco, A.; Venanzi, L. M. *Inorg. Chem.* **1982**, *21*, 4192.

(17) It has been reported that $(Cy_2P(CH_2)_nPCy_2)PtH_2$ (n = 3, 4) complexes show evidence for η^2-dihydrogen behavior, based on variable temperature ^1H NMR spectroscopy: Clark, H. C.; Hampden-Smith, M. J. *J. Am. Chem. Soc.* **1986**, *108*, 3829.

(18) Hasinoff, L.; Takats, J.; Zhang, X. W.; Bond, A. H.; Rogers, R. D. *J. Am. Chem. Soc.* **1994**, *116*, 8833.

$[\{(PMe_3)_3WH_5\}_2Yb(diglyme)]$,[7] in which the P−Yb coupling is *via* a P−M−H- -Yb interaction, as in **5** (assuming that direct Pt−Yb spin−spin communication is negligible, this will be discussed below).

The ^{171}Yb chemical shift of a sample of **1** dissolved in C_6D_6 is −50 ppm ($w_{1/2}$ = 100 Hz), at +60 °C. This is similar to the values reported for $Cp^*_2Yb(thf)_2$ (0 ppm) and $Cp^*_2Yb(Et_2O)_2$ (+36 ppm), both measured at 25 °C.[4b,19] The δ(Yb) value of +572 ppm found for **5** at 25 °C indicates a significantly deshielded ytterbium metal center, relative to that in **1**. Given the few examples of ^{171}Yb chemical shift values reported to date for $Cp^*_2YbL_n$ complexes,[4b,20] the wide variation in these values, and the presence of fast intermolecular exchange of L on the NMR time scale for many of these complexes (the complexes reported in this paper being rare examples of stopped-exchange $Cp^*_2YbL_n$ complexes), a correlation of ^{171}Yb chemical shifts with chemical properties is not yet possible. The ^{195}Pt chemical shift of **5** (−751 ppm) is shifted downfield from the value for **4** (−862 ppm), consistent with less electron density on the platinum center in the adduct. Considering the very large range of platinum chemical shifts (*ca.* 13 000 ppm),[4a] this is not a large perturbation. The Pt−Yb coupling constant, 2260 Hz, is the first transition metal−ytterbium coupling constant to be reported, and so no comparisons can be made. However, it is clear that there is communication between the metal nuclear spins; this will be discussed in more detail below.

To verify the nature of the Lewis acid−base interaction between **1** and **4**, a single crystal X-ray diffraction study was performed on **5**. Unfortunately, the crystal was severely disordered, and only the Yb, Pt, the two P atoms, and rough Cp* ring centroid positions could be located (see the supplementary material for crystallographic details). While the atomic positions have relatively large esd's associated with them, some useful information can nevertheless be obtained. The heavy-atom positions are consistent with a symmetrical $Pt(\mu\text{-}H)_2Yb$ structure, with P(1)−Pt−Yb = 143(1)°, P(2)−Pt−Yb = 137(2)°, and the P−Pt−P plane oriented roughly perpendicular to the (Cp* ring centroid)−Yb−(Cp* ring centroid) plane, the interplanar angle being 86(2)°. The Pt−Yb distance, 3.264(6) Å, is 0.25 Å longer than the sum of the covalent radii (the covalent radii of Pt(II) and Yb(II) are 1.31[21] and 1.70 Å,[22] respectively), indicating that the J_{PtYb} coupling observed in solution is likely not *via* a direct Pt−Yb interaction. This Pt−Yb distance is similar to the W−Yb separation found for $[\{(PMe_3)_3WH_5\}_2Yb(diglyme)]$ (3.24 Å) and to the Nb−Yb separation found for $[\{CpNb(\mu\text{-}H)_2\}_2Yb(diglyme)]$ (3.33 Å) (the van der Waals radii of W and Nb are 1.35 and 1.45 Å, respectively).[7] There has been one previous report of a complex containing both Yb and Pt centers; the Pt−Yb separation in this complex, $[\{Yb(thf)_2(C_5H_4PPh_2)_2Pt(CH_3)_2\}(thf)]$, is 5.01 Å.[23]

Interaction with *cis*-$[(Cy)_2P(CH_2)_3P(Cy)_2]PtH_2$. The energies of the frontier orbitals of a P_2Pt fragment change as the P−Pt−P angle is varied.[24] Specifically, the energy of the P_2Pt HOMO, largely of $d(x^2-y^2)$ character, rises as this angle becomes more acute. Thus, as this angle changes, the Lewis basicity of the hydride ligands of a *cis*-P_2PtH_2 complex would be expected to change. Accordingly, we thought it would be interesting to investigate the interaction of **1** with *cis*-$[(Cy)_2P(CH_2)_3P(Cy)_2]PtH_2$, $(dcypp)PtH_2$ (**6**).[17,25] The P−Pt−P angles in $(dcype)PtH_2$ and $(dcypp)PtH_2$ are *ca.* 87°[26] and 103°,[27] respectively. The NMR spectra of a sample containing a *ca.* 1:1 molar ratio of **1** and **6** (with a slight excess of **1**) indicate that intermolecular exchange is slow on the NMR time scale, at 25 °C. The ^{1}H and ^{31}P{^{1}H} spectra, as well as the ^{1}H/^{195}Pt and ^{1}H/^{171}Yb HMQC spectra (available as supplementary material), were measured on this adduct, **7**, and the spectral values obtained are given in Table 2, along with the values for **6**.

Table 2. ^{1}H, ^{31}P, ^{195}Pt, and ^{171}Yb NMR Data for **6** and **7** (C_6D_6, 25 °C)

	6	**7**
δ(Pt−*H*), ppm	−1.13	−3.45
$^2J_{PH}$(*trans*,*cis*), Hz	+174, −24	+148, −21
$^1J_{PtH}$, Hz	+1069	+993
δ(P), ppm	21.6	15.8
$^1J_{PtP}$, Hz	+1897	+2090
δ(Cp*), ppm		2.44
$^1J_{YbH}$, Hz		+168
J_{YbP}, Hz		+82
δ(Pt), ppm	−861	−749
δ(Yb), ppm		+472
J_{PtYb}, Hz		+2160

Comparing the perturbations resulting from the interaction of **1** with **6** to the perturbations that were observed for **4** (Table 1) shows that they are almost identical. Apparently the interaction between *cis*-P_2PtH_2 complexes and **1** is not significantly affected by a change in the P−Pt−P angle. The two *cis* dihydride complexes, **4** and **6**, also behave similarly with respect to intermolecular exchange with **1**. As found for **4**, an excess of **6** results in averaged spectra, while an excess of **1** does not. The ^{171}Yb chemical shift for **7** is +472 ppm, the analogous value for **5** is +572 ppm; the reason for this difference, and whether it is chemically significant, is unknown. Again, the signs of the coupling constants can be determined and are given in Table 2; the signs are the same as was found for the analogous values for **5**.

Interaction with *cis*-$[(^iPr)_2P(CH_2)_2P(^iPr)_2]Pt(CH_3)_2$. Considering the relatively strong interactions formed between **1** and *cis*-P_2PtH_2 complexes, we wondered whether substitution of the hydrides by methyl groups would result in a similar interaction between the two complexes, *via* bridging methyl groups. The exact nature of the bridging methyl interactions is interesting, specifically whether the methyl groups interact with the Yb center *via* the carbon atoms (M−C−M′ three-center/two-electron interactions), the electron density in the C−H bonds (agostic interactions), or a combination of these two possibilities. Perhaps most interesting is the nature of the interaction in solution, as measured by the methyl-related NMR spectral values, assuming that intermolecular exchange is slow. The dippe analogue, $[(^iPr)_2P(CH_2)_2P(^iPr)_2]Pt(CH_3)_2$ (**8**), was used instead of the dcype derivative, since it crystallizes more readily (the dcype derivative was found to give qualitatively identical NMR spectra as **8**, when combined with **1**).

The complex $(dippe)Pt(\mu\text{-}CH_3)_2YbCp^*_2$ (**9**) is dark green, in contrast to the maroon color of the dihydride complexes.

(19) It is known that ^{171}Yb chemical shifts have a large temperature dependence, see ref 4b.

(20) van den Hende, J. R.; Hitchcock, P. B.; Lappert, M. F.; Nile, T. A. *J. Organomet. Chem.* **1994**, *472*, 79.

(21) Bell, J. D.; Hall, D.; Waters, T. N. *Acta Crystallogr.* **1966**, *21*, 440.

(22) Pauling, L. In *The Nature of the Chemical Bond*, 3rd ed.; Cornell University Press: Ithaca, NY, 1960; pp 260−261.

(23) Deacon, G. B.; Dietrich, A.; Forsyth, C. M.; Schumann, H. *Angew. Chem., Int. Ed. Engl.* **1989**, *28*, 1370.

(24) (a) Hofmann, P.; Heiss, H.; Muller, G. *Z. Naturforsch.* **1987**, *B42*, 395 and references cited therein. (b) Otsuka, S. *J. Organomet. Chem.* **1980**, *200*, 191.

(25) Reference 17 reports that $(dcypp)PtH_2$ exhibits an exchange process between the dihydride and η^2-dihydrogen forms, as determined by variable temperature ^{1}H NMR spectroscopy. We have found that, for (dcypp)-Pt(H)(D), $^1J_{HD}$ is ≤4 Hz at 25 °C, using ^{1}H{^{31}P} NMR spectroscopy.

(26) Hackett, M.; Ibers, J. A.; Whitesides, G. M. *J. Am. Chem. Soc.* **1988**, *110*, 1436.

(27) Barnett, B. L.; Kruger, C.; Tsay, Y.-H. *Chem. Ber.* **1977**, *110*, 3900.

Table 3. ^1H, ^{13}C, and ^{31}P NMR Data for **8** and **9** (C_6D_6, 25 °C)

	8	**9**
$\delta(Pt-CH_3)$, ppm	1.23	0.68
$^2J_{PtCH_3}$, Hz	68	66
$\delta(CH_3)$	18.1	18.0
$^1J_{PtCH_3}$	17.6	17.5
$^1J_{CH_3}$[a]	121	123
δ(P), ppm	70.4	70.0
$^1J_{PtP}$, Hz	1816	1968
δ(Cp*), ppm		2.28
$^1J_{YbH}$, Hz		not observed
J_{YbP}, Hz		not observed

[a] The uncertainty in these values is estimated at ±1 Hz.

Crystals of **9** easily dissolve in toluene (giving a dark green solution), in contrast to the behavior observed for **5**. The room temperature NMR values measured on a sample of **1** and **8** (containing a slight excess of **1**) are shown in Table 3. Intermolecular exchange is rapid on the NMR time scale for this sample. While the intermediate exchange regime can be reached at *ca.* −95 °C in toluene-d_8 (indicated by the presence of broad but distinct resonances for both free and bound Cp* rings), further cooling to −110 °C to try to stop the exchange results in resonances that are too broad to permit the measurement of any coupling constant values (^1H ($w_{1/2}$) = *ca.* 120 Hz).[28] The directions of the perturbations of the spectral values of **9**, relative to those of **8**, are similar to those observed for the dihydride complexes discussed above; however, the extents of the changes are less (Tables 1−3). In the hope of gaining some information concerning the nature of the bridging methyl interaction, the (averaged) C−H coupling constant was measured at 25 °C. The values obtained for **8** and **9** are identical within experimental error; this value is also unchanged at −80 °C. The chemical shift of the methyl carbon nuclei of **9** is also unperturbed, relative to the analogous value for **8** (Table 3). Apparently, the interaction between **1** and **8** in solution is too weak to allow investigation of the methyl−Yb interactions *via* NMR spectroscopy. No low-frequency C−H stretches are present in the solid-state infrared spectrum of **9**.[29]

To gain more information about the details of the Pt−CH_3- -Yb interactions, a single-crystal X-ray diffraction study was performed on **9**. The solid-state structure is shown in Figure 5. This is the first crystallographically characterized complex containing bridging methyl groups between a transition metal and an f-element center. The crystallographic data (Table 4), positional parameters (Table 5), and selected bond distances and angles (Table 6) are presented. Five of the six bridging methyl hydrogens were located from a difference Fourier map, near the end of the structure refinement. The sixth hydrogen, H2C, was added assuming an idealized bonding geometry around C2 (tetrahedral, d(C−H) = 0.95 Å). These atoms were included in the structure factor calculation but not refined. Inclusion of these six hydrogens resulted in a slight improvement in the model, providing confirmation of their positions.

The heavy-atom bonding parameters of **9** are not unusual. The Pt−Yb separation, 4.0391(5) Å, is 0.78 Å longer than the analogous value in **5**. As expected, the methyl groups are symmetrically bridging, with Pt−C(1)−Yb = 106.8(3)°, Pt−C(2)−Yb = 107.5(4)°, and equivalent Pt−C, Pt−P, and Yb−C distances, within experimental error (Table 6); this symmetry introduces a pseudo-C_2 axis through the Pt and Yb metal centers. The Pt−P and Pt−C distances found for **9** are within the expected range for *cis*-$P_2Pt(CH_3)_2$ complexes;[31] no significant perturbations are present as a result of the Yb−methyl interactions. The P(1)−Pt−P(2)/Cp*(1)−Yb−Cp*(2) torsional angle (84.1(4)°), Yb−Cp* distances (2.42 Å for both), and the Cp*(1)−Yb−Cp*(2) angle (139.6(5)°) are within the expected values.

Clearly, the bridging methyl portion of **9** is the structural feature of principal interest. The C(1)−Yb and C(2)−Yb distances are 2.908(8) and 2.88(1) Å, respectively, well within the sum of the van der Waals radii, 3.70 Å (taking the van der Waals radius of a methyl group as 2.00 Å[22]). In Cp*Be(μ-CH_3)YbCp*$_2$, the Yb−methyl carbon distance is 2.766(4) Å, and in $(PPh_3)_2Pt(\mu\text{-}C_2H_4)YbCp^*_2$, the average Yb−C(olefin) distance is 2.781(6) Å.[2d] Based on the orientation of the methyl

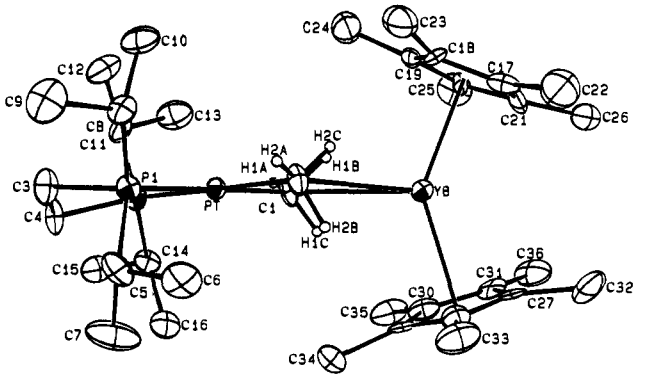

Figure 5. ORTEP diagram of (dippe)Pt(μ-CH_3)$_2$YbCp*$_2$ (**9**) with 50% probability thermal ellipsoids, except for hydrogens.

Table 4. Crystallographic Data for (dippe)Pt(μ-CH_3)$_2$YbCp*$_2$ (**9**)

chem form	$P_2PtYbC_{36}H_{68}$
mol wt	931.02
crystal size (mm)	0.56 × 0.20 × 0.17
T, °C	−125
space group	*C*2/*c*
a, Å	33.90(2)
b, Å	11.255(6)
c, Å	20.535(6)
β, deg	98.41(4)
V, Å^3	7750(7)
Z	8
d(calcd), g cm^{-3}	1.596
μ(calcd), cm^{-1}	61.4
reflns measd	$h,\pm k,+l$
2θ range	3−40°
no. of reflns colld	8420
max correln for cryst decay	2.7% on F
absn corrn[a]	T_{max} = 1.23, T_{min} = 0.825
no. of atoms in least squares	40
no. of unique rflns	3300
no. of reflns with $I > 3\sigma(I)$	6159
p factor	0.03
no. of params	361
R[b]	0.0288
R_w	0.0338
R_{all}	0.0288
GOF	1.168
diff Fourier (e Å^{-3})	+1.0, −0.23

[a] The program DIFABS[30] was used for the absorption correction. [b] The definitions for R and R_w are as follows: $R = f(\Sigma||F_o| - |F_c||,\Sigma|F_o|)$; $R_w = r(f(\Sigma w(|F_o| - |F_c|)^2,\Sigma wF_o^2))$.

(28) We have also tried using fluorinated hydrocarbon solvents and fluorocarbon/toluene solvent mixtures with toluene; however, these attempts have thus far been unsuccessful due to either low solubility of **9** in these solvents or low solubility of these solvents in toluene.

(29) Barnhart, D. M.; Clark, D. L.; Gordon, J. C.; Huffman, J. C.; Watkin, J. G.; Zwick, B. D. *J. Am. Chem. Soc.* **1993**, *115*, 8461. This article reports that the solid- and solution-state IR spectra of $Ln_4(OCH_2{}^tBu)_{12}$ (Ln = La, Nd) contain low-frequency C−H stretches characteristic of Ln- -H−C interactions.

(30) Walker, N.; Stuart, D. *Acta Crystallogr.* **1983**, *A39*, 158.

(31) (a) Kirchner, R. M.; Little, R. G.; Tau, K. D.; Meek, D. W. *J. Organomet. Chem.* **1978**, *149*, C15. (b) Wisner, J. M.; Bartczak, T. J.; Ibers, J. A. *Organometallics* **1986**, *5*, 2044.

Table 5. Atomic Coordinates and *B* Values (Å^2) for the Non-Hydrogen Atoms and H1A–H1C, H2A–H2C of Compound **9**[a]

atom	*x*	*y*	*z*	$B^{b,c}$
PT	−0.13023(1)	−0.38494(1)	−0.00293(1)	1.267(7)
YB	−0.11989(1)	0.14505(1)	−0.14594(1)	1.576(9)
P1	−0.18026(7)	0.4589(2)	0.0464(1)	1.65(5)
P2	−0.08983(7)	0.5173(2)	0.0571(1)	1.57(5)
C1	−0.0843(3)	0.3200(7)	−0.0507(5)	1.8(2)
C2	−0.1671(3)	0.2610(7)	−0.0589(5)	2.0(2)
C3	−0.1593(3)	0.5658(8)	0.1099(5)	2.4(2)
C4	−0.1209(3)	0.6231(8)	0.0962(5)	2.6(2)
C5	−0.2195(3)	0.5434(8)	−0.0043(5)	2.4(2)
C6	−0.2452(3)	0.4687(9)	−0.0558(5)	3.1(3)
C7	−0.2013(3)	0.6443(9)	−0.0385(7)	4.7(3)
C8	−0.2082(3)	0.3525(8)	0.0903(5)	2.0(2)
C9	−0.2356(3).	0.409(1)	0.1346(6)	3.7(3)
C10	−0.1800(3)	0.2615(9)	0.1290(5)	3.1(3)
C11	−0.0547(3)	0.4607(8)	0.1250(5)	2.1(2)
C12	−0.0749(3)	0.388(1)	0.1728(5)	3.5(3)
C13	−0.0212(3)	0.385(1)	0.1027(6)	3.8(3)
C14	−0.0594(3)	0.6110(7)	0.0108(5)	1.8(2)
C15	−0.0361(3)	0.7071(8)	0.0493(5)	2.7(2)
C16	−0.0842(3)	0.6603(8)	−0.0515(5)	2.6(2)
C17	−0.1384(3)	−0.0885(7)	−0.1322(5)	2.3(2)
C18	−0.1352(3)	−0.0424(7)	−0.0683(5)	1.8(2)
C19	−0.0959(3)	−0.0104(7)	−0.0474(5)	2.0(2)
C20	−0.0732(3)	−0.0347(7)	−0.0981(5)	1.8(2)
C21	−0.0981(3)	−0.0843(7)	−0.1506(5)	2.3(2)
C22	−0.1732(3)	−0.144(1)	−0.1738(6)	4.0(3)
C23	−0.1685(3)	−0.0471(8)	−0.0278(6)	3.6(3)
C24	−0.0806(3)	0.0308(9)	0.0211(6)	3.3(3)
C25	−0.0285(3)	−0.0179(9)	−0.0944(6)	3.5(3)
C26	−0.0864(3)	−0.1446(8)	−0.2107(5)	3.3(3)
C27	−0.1361(3)	0.1645(8)	−0.2776(5)	2.7(2)
C28	−0.1596(3)	0.2536(8)	−0.2528(5)	2.1(2)
C29	−0.1322(3)	0.3412(7)	−0.2237(5)	2.0(2)
C30	−0.0936(3)	0.3065(8)	−0.2292(5)	2.4(2)
C31	−0.0963(3)	0.1938(8)	−0.2634(5)	2.1(2)
C32	−0.1539(4)	0.064(1)	−0.3214(6)	4.2(3)
C33	−0.2045(3)	0.259(1)	−0.2631(6)	3.7(3)
C34	−0.1454(3)	0.4600(8)	−0.1970(5)	2.9(2)
C35	−0.0552(3)	0.3711(9)	−0.2073(5)	3.3(3)
C36	−0.0611(3)	0.1302(9)	−0.2848(5)	3.6(3)
H1C	−0.08450(1)	0.33806(1)	−0.09808(1)	2.3*
H1A	−0.05382(1)	0.33927(1)	−0.02860(1)	2.3*
H1B	−0.07878(1)	0.22858(1)	−0.05304(1)	2.3*
H2C	−0.15220(1)	0.18718(1)	−0.05765(1)	2.3*
H2A	−0.19496(1)	0.25005(1)	−0.03780(1)	2.3*
H2B	−0.17414(1)	0.28522(1)	−0.10737(1)	2.3*

[a] Numbers in parentheses give estimated standard deviations. [b] Equivalent isotropic thermal parameters are calculated as $^4/_3[\alpha^2\beta_{11} + b^2\beta_{22} + c^2\beta_{33} + ab(\cos\gamma)\beta_{12} + ac(\cos\beta)\beta_{13} + bc(\cos\alpha)\beta_{23}]$. [c] Starred atoms were included with isotropic thermal parameters.

hydrogens, the interaction involves donation of electron density from the C–H bonds of the methyl groups to the electropositive Yb center (i.e., agostic interactions). The Pt–C–Yb angles, 107° and 108°, are much less acute than the analogous values found for $M(\mu\text{-}CH_3)_2M'$ structures containing M–C–M′ three-center/two-electron type interactions (e.g., $[(CH_3)_3Al]_2$), in which this angle is 75–90°.[32] The analogous angle in $[Cp_2Yb(\mu\text{-}CH_3)]_2$, which contains Yb–C–Yb type bridges, is 86.6°, and the Yb–C distances are 2.49 and 2.54 Å.[33] The Pt–C–Yb angles in **9** are most consistent with agostic C–H- -Yb interactions, as the Pt–C–H angles are *ca.* 106–121°.

For each methyl group, two of the hydrogens are oriented toward the ytterbium center, with distances ranging from 2.30 to 2.63 Å, and one hydrogen is oriented away from the ytterbium center, at a distance of *ca.* 3.8 Å. The van der Waals distance for an Yb- -H interaction is 2.9 Å, using 1.2 Å as the van der Waals radius for a hydrogen atom.[22] The average Yb–H distance in $Cp^*Be(\mu\text{-}CH_3)YbCp^*_2$ is 2.59 (8) Å,[2c] and in $[\{CpNb(\mu\text{-}H)_2\}_2Yb(diglyme)]$, it is 2.33(8) Å.[7] It is informative to compare the bridging methyl interactions of **9** to the C–H- -Yb interactions in $(PPh_3)_2Pt(\mu\text{-}C_2H_4)YbCp^*_2$,[2d] in which the C–Pt–C/C–Yb–C interplanar angle is 15.1°, resulting in two pairs of Yb–H distances (2.58, 2.64 Å; 3.09, 3.15 Å) and two pairs of Yb–C–H angles (69.5°, 100.0°, average values for the short and long Yb–H pairs, respectively). The analogous interplanar angle in **9** is only 4°; however, this also results in two pairs of Yb–H distances (2.30, 2.38 Å; 2.60, 2.63 Å; ignoring the long Yb–H1A, H2A interactions) and also two pairs of Yb–C–H angles (47.9°, 64.2°, average angles for the shorter and longer Yb–H pairs, respectively). While the differences in the pairs of Yb–H interactions are less pronounced than in $(PPh_3)_2Pt(\mu\text{-}C_2H_4)YbCp^*_2$, they are clearly also present for **9**. Given the symmetry of the two complexes, this phenomenon is likely not a steric or crystal packing effect; apparently such pairwise Yb–H interactions are energetically more favorable than four equal Yb–H interactions.

Table 6. Selected Intramolecular Distances (Å) and Angles (deg) in $[(dippe)Pt(\mu\text{-}CH_3)_2YbCp^*_2]$ (**9**)

	Bond Distances		
Pt–Yb	4.0391(5)	Yb–Cp1[a]	2.42
Pt–P1	2.258(3)	Yb–Cp2	2.42
Pt–P2	2.262(2)	Yb–H1A	3.74
Pt–C1	2.089(9)	Yb–H1B	2.38
Pt–C2	2.099(8)	Yb–H1C	2.60
Yb–C1	2.909(8)	Yb–H2A	3.80
Yb–C2	2.88(1)	Yb–H2B	2.63
		Yb–H2C	2.30
	Bond Angles		
P1–Pt–P2	86.97(9)	Cp1–Yb–Cp2	139.6(5)
C1–Pt–C2	86.2(4)	C1–Yb–C2	59.3(2)
Pt–C1–Yb	106.8(3)	Pt–C2–Yb	107.5(4)
Yb–C1–H1A	133.7(6)	Yb–C1–H1B	50.6(4)
Yb–C1–H1C	62.5(4)	Yb–C2–H2A	141.2(6)
Yb–C2–H2B	65.8(5)	Yb–C2–H2C	45.2(5)

[a] All distances and angles involving Cp* rings were calculated using the ring centroid positions, for this structure and also for the structure of **11**.

The orientation of the methyl groups in **9**, with four of the six C–H bonds pointed toward the Yb center, maximizes the amount of electron donation to the Yb center that can occur (as structures containing five and six C–H bonds interacting with the Yb center are clearly chemically unreasonable). This geometry results in an eclipsed geometry of the C–H bonds, relative to the C–C vector (the three pairs of C–Pt–C–H torsional angles for analogous H's are all within 7° of each other). Two *cis*-$L_2M(CH_3)_2$ (M = Pd, Pt) structures have been reported in which the methyl hydrogens have been located;[31b,34] the methyl hydrogens in both of these structures are not eclipsed, relative to the C–C vector. While it is possible that the orientation of the methyl hydrogens in **9** is solely a result of crystal packing and/or steric effects, given the conformations observed in the "free" $L_2M(CH_3)_2$ complexes and the close Yb–H distances in **9**, the observed conformation most likely arises as a result of the agostic C–H- -Yb interactions.

Interaction with *cis*-(dippe)Pt(CH$_3$)(H). It was of interest to see if a methyl hydride complex of platinum would combine the best features of the dihydride and dimethyl complexes, *viz.*, slow intermolecular exchange in solution, while still containing

(32) (a) Tilley, T. D.; Andersen, R. A.; Zalkin, A. *J. Am. Chem. Soc.* **1982**, *104*, 3725 and references cited therein. (b) Stults, S. D.; Andersen, R. A.; Zalkin, A. *J. Organomet. Chem.* **1993**, *462*, 175.

(33) Holton, J.; Lappert, M. F.; Ballard, D. G. H.; Pearce, R.; Atwood, J. L.; Hunter, W. E. *J. Chem. Soc., Chem. Commun.* **1976**, 480.

(34) de Graaf, W.; Boersma, J.; Smeets, W. J. J.; Spek, A. L.; Koten, G. *Organometallics* **1989**, *8*, 2907.

Table 7. ^{1}H, ^{13}C, ^{31}P, ^{195}Pt, and ^{171}Yb NMR Data for **10** and **11** (Toluene-d_8, at 25 and −70 °C)

	25 °C		−70 °C	
	10	**11**	**10**	**11**
δ(Pt−*H*), ppm	0.48	−2.65	0.89	−2.40
$^{2}J_{P\,trans\,H}$, Hz	201	163	198	159
$^{1}J_{PtH}$, Hz	+1158	+1034	+1137	+1020
δ(P), ppm	85.5, 70.1	81.3, 69.2	85.6, 72.0	82.7, 71.2
$^{1}J_{PtP}$, Hz[a]	+1822, +1747	+1978, +2186	+1841, +1775	+1992, +2205
δ(Cp*), ppm	−	2.29, 1.94	−	2.50, 2.06
$^{1}J_{YbH}$, Hz	−	+114	−	+113
J_{YbP}, Hz[a]	−	−, +78	−	−3, +82
δ(CH_3)	1.44	0.64	1.65	0.72
$^{2}J_{PtCH_3}$	−71	−57	−70	−60
J_{YbCH_3}			−	+24
δ(CH_3)			−13.8	−15.4
J_{YbCH_3}			−	+46(4)[b]
$^{1}J_{CH_3}$			121(2)[b]	123(2)[b]
δ(Pt), ppm			−400	−520
δ(Yb), ppm			−	+340
J_{PtYb}, Hz			−	+960

[a] Listed as P *trans* to methyl, P *trans* to hydride, respectively. [b] The estimated uncertainties in these values are shown in parentheses.

a bridging methyl interaction, so that the spectroscopic changes due to the methyl−Yb interaction could be studied. While it has been reported that (dcype)Pt(CH_3)(H) can be synthesized from reaction of (dcype)Pt(CH_3)(Cl) with excess $NaHB(OCH_3)_3$,[35] we found that this method did not work reproducibly, and the yield of the desired product was low when successful. The synthesis of (dmpe)Pt(CH_3)(H) has also been reported, *via* reduction of (dmpe)Pt(CH_3)(OCOPh) with excess $LiHBEt_3$ or $LiBH_4$ at low temperature, although synthetic details were not given.[36] We found that this method is also not reproducible. While it sometimes gave the desired product cleanly, at other times, it gave product mixtures containing many different species, including the desired methyl hydride complex as well as the dihydride complex, the latter presumably arising from reduction of the methyl hydride complex by the excess $LiHBEt_3$/$LiBH_4$. We have found that reaction of (dippe)Pt(CH_3)(OCOPh) with the milder hydride source $NaHB(OCH_3)_3$ in thf results in clean conversion to the desired (dippe)Pt(CH_3)(H) complex, in reproducible yields of 70−80%. This reaction can be done at room temperature, excess $NaHB(OMe)_3$ does not result in product decomposition or reduced yields, and purification of the product is simple (see the Experimental Section for details). It appears that the combination of a milder hydride source, $NaHB(OMe)_3$, with a platinum benzoate complex (containing a better leaving group than the analogous chloride complex) is a better method for synthesis of *cis*-$P_2Pt(CH_3)(H)$ complexes.

Reaction of (dippe)Pt(CH_3)(H) (**10**) with 1 equiv of **1** in toluene results in a beige-orange solution from which dark green-brown crystals, formulated as (dippe)Pt(μ-CH_3)(μ-H)$YbCp^*_2$ (**11**), can be isolated in 70% yield. The crystals are solvent-loss sensitive and turn gold upon exposure to vacuum. This solid has a ν(M−H) band at 1895 cm^{-1} in its solid-state infrared spectrum, shifted from 1965 cm^{-1} for **10**. As found for **9**, no low-frequency C−H stretches are present in the infrared spectrum, and crystals of **11** redissolve in toluene. A sample of this solid dissolved in C_6D_6 gives NMR spectra that indicate intermolecular exchange is rapid at 25 °C; no coupling to ^{171}Yb is observed, and broadened resonances are present. However, a toluene-d_8 solution of **1** and **10**, containing a slight excess of **1**, does not show intermolecular exchange at 25 °C, presumably for the same reasons as mentioned above (Figure 2 and accompanying discussion). Coupling of ^{171}Yb to the hydride as well as to the phosphorus nucleus that is *trans* to the hydride is present at 25 °C. However, coupling to ^{171}Yb is not resolved for the methyl platinum-related resonances, in the room temperature 1-D ^{1}H and $^{31}P\{^{1}H\}$ (P *trans* to the methyl group) NMR spectra. The NMR values measured on this sample at 25 and −70 °C are given in Table 7.

Considering first the room temperature ^{1}H and ^{31}P data, the perturbations in the values resulting from the presence of **1** are roughly equivalent to the changes that were seen for the analogous values in the dihydride and dimethyl complexes (Tables 1−3). Both $^{1}J_{YbH}$ and J_{YbP} (for the P *trans* to the hydride) are slightly smaller for **11**, indicative of a slightly weaker Yb−hydride interaction in **11** than in the dihydride complexes **5** and **7**. This may be a result of steric interactions between the Yb center and the methyl group, preventing the Yb center from approaching the hydride ligand as closely as in the dihydride complexes. Both the ^{1}H chemical shift perturbation of the methyl protons ($\Delta(\delta)$ = 0.55 ppm for **9**, 0.80 ppm for **11**), as well as the $^{2}J_{PtCH_3}$ perturbation ($\Delta(J)$ = 2 Hz for **9**, 14 Hz for **11**), are larger than for **9**, presumably indicating a stronger Yb- -CH_3 interaction in **11**, relative to that in **9**.

The ^{1}H and ^{31}P NMR values of **11** are relatively unchanged upon cooling to −70 °C, suggesting that the nature of the interaction between **1** and **10** is not changed significantly over this temperature range. The $^{1}H/^{195}Pt$ HMQC spectrum measured at −70 °C (available as supplementary material) shows the presence of spin−spin coupling between ^{195}Pt and ^{171}Yb (J_{PtYb} = 960 Hz) of roughly one-half the size of the analogous values measured for **5** and **7**. The ^{195}Pt chemical shift is shifted upfield from the value for **10** ($\Delta(\delta)$ = −120 ppm), in contrast to the downfield shifts observed for **5** and **7** ($\Delta(\delta)$ = +111 and +112 ppm, respectively). The ^{171}Yb shift for **11** at −70 °C is +340 ppm, shifted downfield 390 ppm from free **1**. This contrasts with a downfield shift of 622 ppm for **5** and 522 ppm for **7**, perhaps indicative of a weaker interaction between **1** and **10**, relative to the interactions formed between **1** and the *cis* dihydride complexes.

The $^{1}H/^{195}Pt$ spectrum of **11** at 0 °C (Figure 6) shows that at this temperature J_{PtYb} is identical to the value obtained at −70 °C (this spectrum was optimized for the $^{2}J_{PtH}$ of the methyl protons, 58 Hz).

In addition, coupling of the ytterbium center to the methyl hydrogens is observed, J_{YbCH_3} = 24 Hz. This value was also measured at −70 °C and was found to be identical. These similar spectroscopic values for **11** at 0 and −70 °C show that

(35) Hackett, M.; Whitesides, G. M. *J. Am. Chem. Soc.* **1988**, *110*, 1449.
(36) Alcock, N. W.; Brown, J. M.; MacLean, T. D. *J. Chem. Soc., Chem. Commun.* **1984**, 1689.

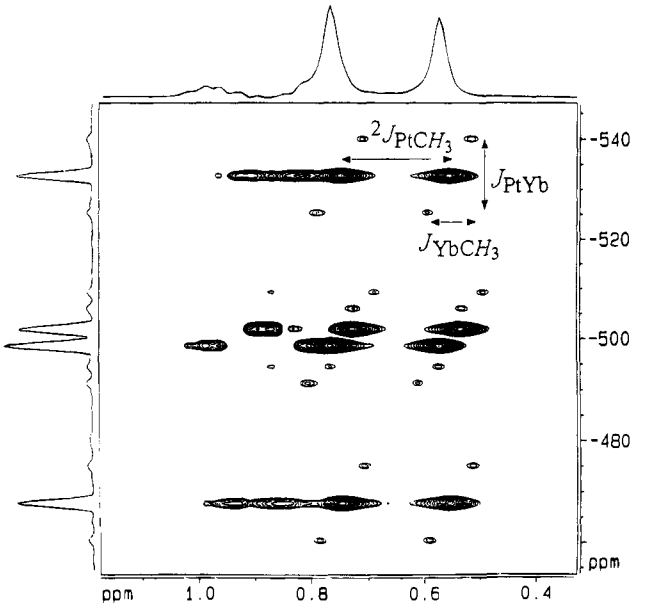

Figure 6. $^1H/^{195}Pt$ HMQC NMR spectrum of **11** (300 MHz, toluene-d_8, 0 °C), showing the methyl−platinum cross peak region. Extra correlations are visible to the dippe ligand protons. Annotated with ^1H and ^{195}Pt projections in F2 and F1, respectively.

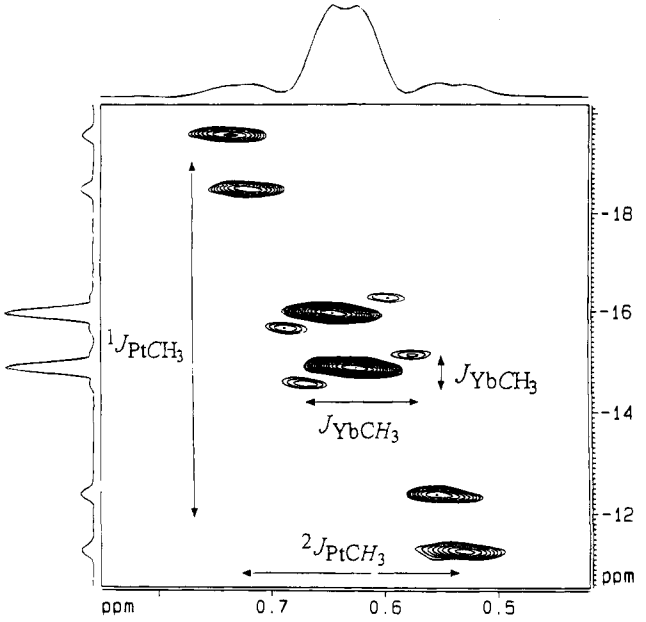

Figure 7. $^1H/^{13}C$ HSQC NMR spectrum of **11** (300 MHz, toluene-d_8, −70 °C), showing the methyl region. ^{171}Yb satellites are visible only for the major resonance and not for the ^{195}Pt satellites, due to insufficient signal/noise. Annotated with ^1H and ^{13}C projections in F2 and F1, respectively.

the nature of the interaction is largely unchanged within this temperature range, as suggested by the ^1H and ^{31}P data. It is clear from Figure 6 why J_{YbCH_3} is not visible in the 1-D ^1H spectrum of **11**: it is obscured by the methyl resonance of the non-^{171}Yb isotopomers. Use of the $^1H-^{195}Pt$ HMQC however, makes use of the large $^{195}Pt-^{171}Yb$ coupling to generate the E.COSY-like pattern,[13] allowing elucidation of $^1J_{YbCH_3}$.

On the basis of the 24 Hz value of J_{YbCH_3}, there is clearly an Yb- -CH_3 interaction present. A $^1H/^{31}P$ HMQC spectrum of **11** acquired at −70 °C shows coupling of ^{171}Yb to the phosphorus nucleus *trans* to the methyl group, of *ca.* 3 Hz (this spectrum is available as supplementary material). This coupling is not seen in the 1-D $^{31}P\{^1H\}$ spectrum, as it is within the line width of the major resonance. This coupling is much smaller than the analogous coupling to the phosphorus nucleus that is *trans* to the hydride ligand, 82 Hz. In a similar manner, the $^1H/^{13}C$ HSQC[37] spectrum shown in Figure 7 (optimized for $^1J_{CH_3}$ = 123 Hz) allows the measurement of J_{YbCH_3}, 46 ± 4 Hz.

As was found for **9**, the $^1J_{CH_3}$ coupling constant for the bridging methyl group of **11** is unchanged from that of free **10**. As the signs of $^1J_{PtH}$, $^1J_{PtC}$, $^1J_{PtP}$ are all positive,[14] the signs of the rest of the coupling constants can be obtained from the 2-D spectra (including the $^1H/^{195}Pt$ spectrum at −70 °C, available as supplementary material); these signs are given in Table 7.

An X-ray structure determination was performed on **11** in order to investigate the details of the interaction between **1** and **10** in the solid state. The crystallographic data (Table 8), positional parameters (Table 9), and selected intramolecular distances and angles (Table 10) are given below.

Unfortunately, three of the four isopropyl groups are disordered, as are both of the Cp* rings. While this disorder was satisfactorily modeled (see the Experimental Section for details), the hydrogen atoms on the bridging methyl group, as well as the hydride ligand, could not be located in the Fourier difference map. Nevertheless, the core of the structure is well-defined (Figure 8) and yields some valuable information.

While the hydride ligand was not found, its location is clear from the square planar coordination about the Pt center. The Pt−Yb separation is 3.388(9) Å, compared to 3.264 Å for **5** and 4.039 Å for **9**. The P−Pt−Yb angles (P(1)−Pt−Yb = 145.8(1)°, P(2)−Pt−Yb = 127.2(1)°) show that the (μ-CH_3)-(μ-H) bridge is asymmetric, with the Yb center pulled toward the hydride. The Pt−P distances are equivalent within experimental error (Pt−P(1) = 2.256(5) Å, Pt−P(2) = 2.252(5) Å) and are identical within experimental error to those found for **9**. The normally higher *trans* influence of the hydride ligand relative to an alkyl group[38] is absent, likely a result of the stronger Yb−hydride interaction *vs* the Yb−methyl interaction. The Pt−methyl carbon distance in **11** (2.16(2) Å) is identical

Table 8. Crystallographic Data for [dippe)Pt(μ-CH_3)(μ-H)YbCp*$_2$] (**11**)

chem form	$P_2PtYbC_{35}H_{66}$
mol wt	916.99
crystal size (mm)	0.40 × 0.35 × 0.26
T, °C	−100
space group	$P2_1/c$
a, Å	18.778(5)
b, Å	10.903(4)
c, Å	20.255(5)
β, deg	114.74(2)
V, Å^3	3766(2)
Z	4
d(calcd), g cm^{-3}	1.617
μ(calcd), cm^{-1}	63.1
reflns measd	$h,\pm k,+l$
2θ range	3−55°
no. of reflns collected	7390
max correl for cryst decay	not done
absn corrn[a]	T_{max} = 2.00, T_{min} = 0.696
no. of atoms in least squares	59
no. of unique reflns	6669
no. of reflns with $I > 3\sigma(I)$	4710
p factor	0.05
no. of params	327
R	0.0689
R_w	0.0815
R_{all}	0.103
GOF	2.179
diff Fourier (e Å^{-3})	+6.6,[b] −0.47

[a] The program DIFABS[30] was used for the absorption correction. [b] See X-ray summary in the Experimental Section.

(37) Bodenhausen, G.; Ruben, D. *J. Chem. Phys. Lett.* **1980**, *69*, 185.

Table 9. Atomic Coordinates and B Values (Å^2) for the Non-Hydrogen Atoms of Compound **11**[a]

atom	x	y	z	B[b]
Pt	0.72996(1)	0.38180(1)	0.03830(1)	3.23(1)
Yb	0.74825(1)	0.57953(1)	−0.08271(1)	2.99(1)
P1	0.6471(3)	0.2962(4)	0.0798(2)	4.4(1)
P2	0.8255(3)	0.2693(5)	0.1225(2)	4.5(1)
C1	0.774(2)	0.549(4)	−0.206(2)	6.1(9)*
C1a	0.793(2)	0.509(2)	−0.183(1)	2.7(5)*
C2	0.711(1)	0.556(2)	−0.2259(7)	5.1(4)
C3	0.6637(9)	0.472(2)	−0.2136(7)	4.3(4)
C4	0.712(1)	0.377(2)	−0.1701(7)	4.8(4)
C5	0.787(1)	0.418(2)	−0.1596(9)	6.1(5)
C6	0.872(2)	0.565(3)	−0.183(2)	6.6(8)*
C6a	0.831(3)	0.631(4)	−0.222(2)	4(1)*
C7	0.704(2)	0.664(3)	−0.274(2)	6.7(7)*
C7a	0.643(3)	0.656(4)	−0.286(2)	3.8(9)*
C8	0.576(2)	0.493(3)	−0.252(1)	5.6(6)*
C8a	0.575(3)	0.431(5)	−0.232(2)	4(1)*
C9	0.672(1)	0.264(2)	−0.152(1)	4.2(5)*
C9a	0.730(3)	0.249(5)	−0.134(2)	4(1)*
C10	0.856(2)	0.308(3)	−0.106(1)	6.1(7)*
C10a	0.882(3)	0.383(5)	−0.125(3)	5(1)*
C11a	0.852(2)	0.768(3)	−0.040(2)	4.1(7)*
C11	0.847(2)	0.757(2)	−0.005(1)	2.4(5)*
C12	0.7911(9)	0.814(1)	−0.0837(8)	4.2(4)
C13	0.7240(9)	0.819(1)	−0.072(1)	4.7(5)
C14	0.732(1)	0.778(2)	−0.009(1)	3.9(5)*
C15a	0.786(1)	0.747(2)	0.025(1)	3.5(4)*
C15	0.839(2)	0.739(3)	0.023(1)	6.0(7)*
C16	0.934(2)	0.739(4)	0.022(2)	5.8(9)*
C16a	0.911(3)	0.684(5)	0.093(2)	8(1)*
C17	0.777(2)	0.895(4)	−0.165(2)	6.0(9)*
C17a	0.828(2)	0.867(4)	−0.130(2)	5.7(9)*
C18	0.650(2)	0.878(3)	−0.141(2)	4.4(7)*
C18a	0.645(2)	0.867(4)	−0.093(2)	5.5(8)*
C19	0.650(2)	0.794(4)	0.006(2)	6(1)*
C19a	0.722(3)	0.755(4)	0.062(2)	7(1)*
C20	0.825(2)	0.706(3)	0.109(1)	3.8(6)*
C20a	0.932(3)	0.772(4)	−0.044(2)	7(1)*
C21	0.696(2)	0.178(3)	0.141(1)	3.2(5)*
C21a	0.711(2)	0.225(3)	0.174(1)	3.1(5)*
C22	0.774(2)	0.144(4)	0.159(2)	5.7(9)*
C22a	0.791(2)	0.201(3)	0.183(2)	4.5(7)*
C23	0.593(1)	0.403(2)	0.1120(8)	5.1(5)
C24	0.653(1)	0.505(2)	0.158(1)	8.2(6)
C25	0.549(1)	0.342(2)	0.151(1)	7.0(6)
C26	0.559(2)	0.204(3)	0.007(1)	6.3(7)*
C26a	0.574(3)	0.177(4)	0.042(2)	3.8(9)*
C27	0.493(2)	0.275(4)	−0.048(2)	8.1(9)*
C27a	0.524(4)	0.218(6)	−0.041(3)	7(2)*
C28	0.594(3)	0.117(4)	−0.029(2)	10(1)*
C28a	0.612(4)	0.060(6)	0.036(3)	7(2)*
C29	0.880(1)	0.158(2)	0.092(1)	5.5(5)*
C30	0.817(2)	0.069(2)	0.031(1)	9.2(8)
C31	0.945(2)	0.076(4)	0.147(2)	6.0(9)*
C31a	0.930(2)	0.217(4)	0.064(2)	7(1)*
C32	0.903(2)	0.354(2)	0.192(1)	8.1(7)
C33	0.869(1)	0.448(3)	0.230(1)	10.9(9)
C34	0.967(2)	0.295(4)	0.245(2)	6(1)*
C34a	0.952(3)	0.414(4)	0.163(2)	7(1)*
C35	0.636(1)	0.491(2)	−0.0388(8)	4.7(5)

[a] Numbers in parentheses give estimated standard deviations. [b] Starred atoms were included with isotropic thermal parameters.

within experimental error to the analogous distances found for **9** (2.089(9) and 2.099(8) Å). The P(1)−Pt−P(2)/Cp*(1)−Yb−Cp*(2) torsional angle (92(2)°), Yb−Cp* distances (2.41 and 2.43 Å), and Cp*−Yb−Cp* angle (137(1)°) are normal. The Pt−C(35)−Yb angle of 85° contrasts with the analogous values for **9** (107° and 108°) and shows the asymmetry of the bridge.

(38) Hackett, M.; Ibers, J. A.; Jernakoff, P.; Whitesides, G. M. *J. Am. Chem. Soc.* **1986**, *108*, 8094. This paper reports that, for the solid-state structure of (dcype)Pt($CH_2C(CH_3)_3$(H), the Pt−P distances are 2.278(2) Å (*trans* to hydride) and 2.253(2) Å (*trans* to alkyl group), respectively.

Table 10. Selected Intramolecular Distances (Å) and Angles (deg) in [(dippe)Pt(μ-CH_3)(μ-H)YbCp*$_2$] (**11**)

	Bond Distances		
Pt−Yb	3.388(9)	Yb−Cp1	2.43
Pt−P1	2.256(5)	Yb−Cp2	2.41
Pt−P2	2.252(5)	Yb−C35	2.79(2)
Pt−C35	2.16(2)		
	Bond Angles		
P1−Pt−P2	87.0(2)	Cp1−Yb−Cp2	137(1)
Pt−C35−Yb	85.4(6)	P1−Pt−Yb	145.8(1)
P2−Pt−Yb	127.2(1)		

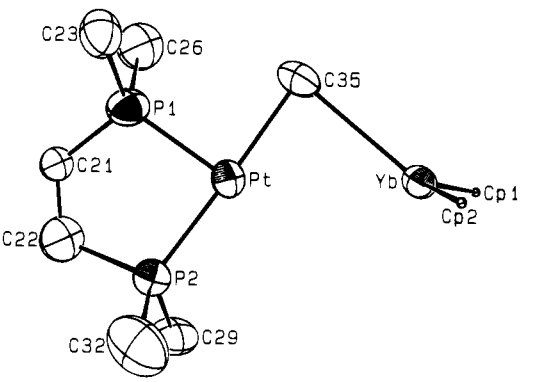

Figure 8. ORTEP diagram of (dippe)Pt(μ-H)(μ-CH_3)YbCp*$_2$ (**11**) with 50% probability thermal ellipsoids. For clarity, the disordered isopropyl groups and Cp* rings are not shown (the Cp* ring centroid positions are shown).

This angle is within the range normally found for M(μ-CH_3)$_2$M′ structures possessing M−C−M′ three-center/two-electron type interactions.[32]

Discussion

The results presented above show that *cis*-P_2PtH_2 and *cis*-$P_2Pt(CH_3)(H)$ complexes form interactions of significant strength with the bent metallocene Cp*$_2$Yb. It is clear that a hydride is a better ligand toward **1** than a methyl group. Strictly speaking, the exchange behavior observed for **9** indicates that the kinetic barrier for the interaction of **1** with **8** is small, relative to the barrier for the dihydride (and methyl hydride) complexes. Given the bent geometry of **1** and the overall lack of structural changes in general upon forming the Lewis acid−base adducts from **1** and the *cis*-P_2PtX_2 complexes, it is reasonable to assume that this barrier gives a qualitative indication of the strength of the interaction. Thus, the higher barriers for **5** and **7** (slow exchange), relative to the smaller barrier for **9** (fast intermolecular exchange), is consistent with a Yb−hydride interaction that is thermodynamically stronger than a Yb−methyl interaction. The unchanged methyl C−H coupling constant and lack of any low-frequency C−H stretches in the solid-state infrared spectrum of **9** are further indications that the agostic interactions are relatively weak and do not significantly perturb the C−H bond, in either the solution or solid state.

The solid-state structural parameters for **11** are consistent with a Pt−C−Yb interaction, in contrast to the agostic interactions observed in the solid state for **9**. Also consistent with Pt−C−Yb interactions in **11** is the Pt−Yb distance, 3.388(1) Å, only 0.12 Å longer than the analogous distance for **5** and 0.65 Å shorter than the distance found for **9**. Whether the agostic interactions in **9** are more favorable energetically than the direct C−Yb interaction in **11** is unknown. If the former are more

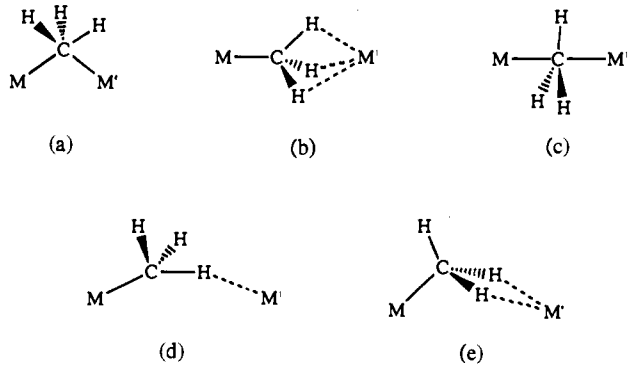

Figure 9. Different types of bridging methyl groups that have been crystallographically characterized.

favorable, then the Pt−C−Yb interaction observed for **11** can be rationalized by assuming that the much stronger Yb−hydride interaction results in an asymmetric bridge, giving the Yb center no choice but to form a direct C−Yb interaction.

The agostic interactions observed in the solid-state structure of **9** represent a rare bonding mode for bridging methyl groups. The different orientations of bridging methyl groups that have been structurally characterized are shown in Figure 9.

The most common orientation observed is the M−C−M′ type (Figure 9a),[33,39] the classic example being the trimethylaluminum dimer.[40] Several examples of types b,[2c,41] c,[42] and d[43] have also been observed. To the best of our knowledge, only two examples of type e, the orientation observed for **9**, have been reported.[44]

Unfortunately, the solution NMR data for **11** do not give a clear answer with respect to distinguishing between agostic interactions, a Yb−C interaction, or a combination of both (phenomenologically, a bridging alkyl augmented by an α-agostic interaction).[45] The coupling of ^{171}Yb to both the C and H nuclei of the bridging methyl group in **11** is consistent with all three of these possibilities,[47] as is the unchanged $^1J_{CH_3}$ value for **11**. It is known that $^1J_{CH_3}$ values are not significantly perturbed upon formation of M−C−M′ bridging interactions.[48] There have also been several reports of agostic complexes in which $^1J_{CH}$ is unchanged or decreases only very slightly (see below).[49] The observation that J_{YbCH_3} and J_{YbCH_3} for **11** have the same signs does not unequivocally rule out a direct Yb−C interaction. While $^1J_{MC}$ and $^2J_{MCH_3}$ generally have opposite signs for transition metal complexes containing direct M−C interactions (where M is an NMR-active isotope),[50] the small number of these examples requires that the sign criterion be used critically. However, the same signs of J_{YbCH_3} and J_{YbCH_3} for **11** are certainly *least* consistent with *just* a direct Yb−C interaction.

Comparison of the $J_{YbC,H}$ values measured on **11** to $J_{MC,H}$ values of bridging hydride and methyl complexes that have been reported in the literature is also informative. While J_{YbH} and J_{YbC} values cannot be measured on $[Cp_2Yb(\mu\text{-}CH_3)]_2$, a compound with a Yb−C−Yb interaction in the solid state[32,51] (Yb(III) is paramagnetic), both J_{YH} and J_{YC} have been measured for $[Cp_2Y(\mu\text{-}CH_3)]_2$, which also possesses M−C−M bridges in the solid state.[51] The $^1J_{YC}$ value for this complex is 25.0 Hz, while J_{YH} is 3.6 Hz (all of the $J_{YC,H}$ values discussed in this paragraph are absolute values, as the signs of the coupling constants have not been reported), consistent with a direct Y−C interaction and longer range (two-bond) Y−H interactions; this gives a ratio of J_{YC}/J_{YH} of 6.94. The ratio for $Cp_2Y(\mu\text{-}CH_3)_2\text{-}Al(CH_3)_2$,[52] which also has M−C−M′ type interactions in the solid state,[39] is J_{YC}/J_{YH} = 12.2 Hz/5.0 Hz = 2.44. For **11**, the analogous ratio is J_{YbC}/J_{YbH} = 46 Hz/24 Hz = 1.92 (the use of reduced coupling constants, K, is not necessary, as the nuclei being compared are constant). It is also interesting to compare the J_{YH} value of 3.6 Hz for $[Cp_2Y(\mu\text{-}CH_3)]_2$ to the J_{YH} values found for $(Cp_2(thf)Y(\mu\text{-}H)]_2$ (27.0 Hz)[53] and $[Cp^*_2Y(\mu\text{-}H)]_2$ (37.5 Hz),[54] giving [J_{YH} (μ-H complex)/J_{YH}(μ-CH_3 complex)] ratios of 7.50 and 10.4, respectively. The analogous values for the Yb complexes, **11** and **5**, give a ratio of 180 Hz/24 Hz = 7.50.

The J_{PtH} and J_{PtC} values have been measured for a series of *trans*-$PtCl_2LX$ complexes (L = PR_3, AsR_3, olefin; X = a quinoline/Schiff base derivative, possessing an aryl/alkyl donor C−H bond(s)).[49b] These complexes have been described as "weak" agostic complexes. They are square planar Pd, Pt, or

(39) Holton, J.; Lappert, M. F.; Scollary, G. R.; Ballard, D. G. H.; Pearce, R.; Atwood, J. L.; Hunter, W. E. *J. Chem. Soc., Chem. Commun.* **1976**, 425.

(40) (a) Lewis, P. H.; Rundle, R. E. *J. Chem. Phys.* **1953**, *21*, 986. (b) Vranka, R. G.; Amma, E. L. *J. Am. Chem. Soc.* **1967**, *89*, 3121. (c) Huffman, J. C.; Streib, W. E. *J. Chem. Soc., Chem. Commun.* **1971**, 911.

(41) (a) Watson, P. L.; Parshall, G. W. *Acc. Chem. Res.* **1985**, *18*, 51. (b) Busch, M. A.; Harlow, R.; Watson, P. L. *Inorg. Chim. Acta* **1987**, *140*, 15. (c) Hitchcock, P. B.; Lappert, M. F.; Smith, R. C. *J. Chem. Soc., Chem. Commun.* **1989**, 369.

(42) (a) Waymouth, R. M.; Santarsiero, B. D.; Coots, R. J.; Bronikowski, M. J.; Grubbs, R. H. *J. Am. Chem. Soc.* **1986**, *108*, 1427. (b) Waymouth, R. M.; Santarsiero, B. D.; Grubbs, R. H. *J. Am. Chem. Soc.* **1984**, *106*, 4050. (c) Waymouth, R. M.; Potter, K. S.; Schaeffer, W. P.; Grubbs, R. H. *Organometallics* **1990**, 2843.

(43) (a) Ozawa, F.; Park, J. W.; Mackenzie, P. B.; Schaefer, W. P.; Henling, L. M.; Grubbs, R. H. *J. Am. Chem. Soc.* **1989**, *111*, 1319. (b) Park, J. W.; Mackenzie, P. B.; Schaefer, W. P.; Grubbs, R. H. *J. Am. Chem. Soc.* **1986**, *108*, 6402. (c) Dawkins, G. M.; Green, M.; Orpen, A. G.; Stone, F. G. A. *J. Chem. Soc., Chem. Commun.* **1982**, 41.

(44) (a) Hitchcock, P. B.; Howard, J. A. K.; Lappert, M. F.; Prashar, S. *J. Organomet. Chem.* **1992**, *437*, 177. (b) Yang, X.; Stern, C. L.; Marks, T. J. *J. Am. Chem. Soc.* **1991**, *113*, 3623.

(45) While isotopic perturbation of resonance/coupling constant experiments may be informative,[46] given the small perturbations in the methyl-related spectral values for **10** relative to those of **11**, such experiments will likely give ambiguous results (see especially ref 46a below). Related to this, the J_{YbCH_3} value will not change very much upon partial deuteration of the methyl group. If it is assumed that two methyl hydrogens interact with the Yb center, then the *maximum* value for J_{YbCDH_2} for (dippe)Pt(μ-CDH_2)(μ-H)YbCp^*_2 would be 36 Hz. This maximum value would be observed only if the methyl group were not rotating, with both hydrogens oriented toward the Yb center, an unlikely scenario.

(46) (a) Green, M. L. H.; Hughes, A. K.; Popham, N. A.; Stephens, A. H. H.; Wong, L.-L. *J. Chem. Soc., Dalton Trans.* **1992**, 3077. (b) Calvert, R. B.; Shapley, J. R. *J. Am. Chem. Soc.* **1978**, *100*, 7726. (c) Casey, C. P.; Fagan, P. J.; Miles, W. H. *J. Am. Chem. Soc.* **1982**, *104*, 1134.

(47) Recently (Hitchcock, P. B.; Holmes, S. A.; Lappert, M. F.; Tian, S. *J. Chem. Soc., Chem. Commun.* **1994**, 2691), a $^2J_{YbH}$ value of 30 Hz has been reported for $[Yb[CH(SiMe_3)_2]_2(OEt_2)_2]$ and a $^1J_{YbC}$ value of 0.32 Hz has been reported for $[Yb\{N(SiMe_3)C(^tBu)CH(SiMe_3)\}_2]$. The $^2J_{YbH}$ value is similar to that measured for **11**; however, the $^1J_{YbC}$ value is much smaller than the analogous value for **11** and is unexpectedly small for a one-bond Yb−C coupling constant.

(48) For example, $^1J_{CH_3}$ values for the terminal and bridging methyl groups of $[(CH_3)_3Al]_2$ are 112.7 and 115.3 Hz, respectively (Olah, G. A.; Prakash, K. S.; Liang, G.; Henold, K. L.; Haigh, G. B. *Proc. Natl. Acad. Sci. U.S.A.* **1977**, *74*, 5217).

(49) (a) Neve, F.; Ghedini, M.; Crispini, A. *Organometallics* **1992**, *11*, 3324. (b) Albinati, A.; Pregosin, P. S.; Wombacher, F. *Inorg. Chem.* **1990**, *29*, 1812. (c) Albinati, A.; Anklin, C. G.; Ganazoli, F.; Ruegg, H.; Pregosin, P. S. *Inorg. Chem.* **1987**, *26*, 503. (d) Albinati, A.; Arz, C.; Pregosin, P. S. *Inorg. Chem.* **1987**, *26*, 508. (e) Anklin, C. G.; Pregosin, P. S. *Magn. Reson. Chem.* **1985**, *23*, 671. (f) Deeming, A. J.; Rothwell, I. P.; Hursthouse, M. B.; Abdul Malik, K. M. *J. Chem. Soc., Dalton Trans.* **1980**, *1974*.

(50) Jameson, C. J. In *Multinuclear NMR;* Mason, J., Ed.; Plenum Press: New York, 1987; pp 106−109.

(51) Holton, J.; Lappert, M. F.; Ballard, D. G. H.; Pearce, R.; Atwood, J. L.; Hunter, W. E. *J. Chem. Soc., Dalton Trans.* **1979**, 54.

(52) Holton, J.; Lappert, M. F.; Ballard, D. G. H.; Pearce, R.; Atwood, J. L.; Hunter, W. E. *J. Chem. Soc., Dalton Trans.* **1979**, 45.

(53) Evans, W. J.; Meadows, J. H.; Wayda, A. L.; Hunter, W. E.; Atwood, J. L. *J. Am. Chem. Soc.* **1982**, *104*, 2008.

(54) Booij, M.; Deelman, B.-J.; Duchateau, R.; Postma, D. S.; Meetsma, A.; Teuben, J. H. *Organometallics* **1993**, *12*, 3531.

Rh complexes containing the agostic donor held rigidly in place in the pseudoaxial fifth coordination site, and they have an unperturbed $^1J_{CH}$ value and a low-field shift of the agostic hydrogen resonance, in contrast to the high-field shift that is commonly observed for agostic complexes.[49] The J_{PtC}/J_{PtH} values for these complexes are in the range of *ca.* 2.3−3.2, similar to the value observed for **11**. It is interesting that for [*trans*-Rh(CO)(8-methylquinoline)$(PPh_3)_2$][BF_4],[49a] which also contains a weak agostic interaction, J_{RhC} is 1.8 Hz while J_{RhH} is not observed. To the best of our knowledge, the only example of a "true" agostic complex for which J_{MC} and J_{MH} have been measured is [(Cp*)Rh($C_{10}H_{13}$)][PF_6] (in which $^1J_{CH}$ is 83 Hz, lowered from 152 Hz);[55] the measured values give a J_{RhC}/J_{RhH} ratio of 3.6 Hz/10.2 Hz = 0.35,[56] far lower than the value observed for **11**.[57] On the basis of the coupling constant ratios in this diverse set of compounds and the unchanged $^1J_{CH_3}$ value in **11**, it is reasonable to classify **11** as a weak agostic complex in solution.[58]

The strong Yb−hydride interaction in **11** results in a close Yb−CH_3 contact and the observed Yb- -methyl interactions. This is similar to the weak agostic complexes mentioned above, in which the C−H donor is held rigidly near the metal center. The agostic interactions in this class of complexes, and likely also in **11**, are mainly a result of geometrical constraints; these geometrical constraints (i.e., the exact orientation of the metal center relative to the C−H donor(s)) determine the details of the agostic interaction. This is in contrast to "classical" or "strong" agostic complexes, in which the interaction arises mainly from orbital energy considerations. The distinction between "classical" and "weak" agostic complexes is not unambiguous; the latter class is characterized by unchanged $^1J_{CH}$ values and J_{MC}/J_{MH} ratios intermediate between M−C−M′ type complexes and agostic complexes in which $^1J_{CH}$ is substantially lowered.

The presence of coupling between the Pt and Yb centers in **5**, **7**, and **11** indicates that there is communication of the metal nuclear spins, likely *via* the bridging ligands. Is this Pt−Yb nuclear spin−spin communication significant? As mentioned above, there have not been many J_{YbX} values reported and no Yb−transition metal coupling constants. Comparison of the reported J_{YbX} values to the J_{PtYb} values measured for **5**, **7**, and **11** is not valid, as different nuclei are involved, and the different magnetogyric ratios make such a comparison meaningless. Comparision of the reduced coupling constant values is complicated by the fact that, while such values are independent of the magnetogyric ratios involved, they are still dependent on the atomic number and are also strongly affected by relativistic effects, which will be large for both ^{195}Pt and ^{171}Yb.[59] It is known that J_{PtPt} values for polynuclear Pt complexes show no correlation with solid-state Pt−Pt distances and a similar possibility has been suggested for J_{PtW} values.[14] Another potential complication is the possibility of two different communication mechanisms, a direct Pt−Yb interaction and interaction *via* the bridging ligands. The coupling *via* the first mechanism (one-bond) may be either of the same or of opposite sign to the coupling *via* the second mechanism (>one-bond), and this can have a large effect on the measured coupling constant value; this has been suggested as a possible reason for the seemingly random J_{PtPt} values.[14] Consequently, the only thing that can be stated with certainty concerning the J_{PtYb} values measured on **5**, **7**, and **11** is that there is nuclear spin communication between the metal centers and that this communication is about equal for **5** and **7** and roughly halved for **11**. Whether the difference is a consequence of the different bridging ligands in the complexes, of the longer Pt−Yb separation for **11**, or a combination of these two possibilities is unknown.

(55) Bennett, M. A.; McMahon, I. J.; Pelling, S.; Robertson, G. B.; Wickramasinghe, W. A. *Organometallics* **1985**, *4*, 754.

(56) Ball, G. E. Unpublished results.

(57) Two examples of Pt(II) complexes containing β-agostic CH_3 interactions, in which rotation about the $C_\alpha-C_{agostic}$ bond can be frozen out, have been reported (Carr, N.; Mole, L.; Orpen, A. G.; Spencer, J. L. *J. Chem. Soc., Dalton Trans.* **1992**, 2653); unfortunately, the coupling constants between the agostic C and H nuclei and the Pt center were not reported.

(58) The $\delta(CH_3)$ resonance for **11** is shifted upfield, relative to the analogous value in **10**. Reference 49b contains a discussion concerning the origin of the low-field ^{1}H shifts for weak agostic complexes.

(59) Sanders, J. C. P.; Schrobilgen, G. J. In *Multinuclear Magnetic Resonance in Liquids and Solids−Chemical Applications;* Granger, P., Harris, R. K., Eds.; Kluwer Academic Publishers: Dordrecht, The Netherlands, 1990; Chapter XI.

Conclusion

We have found that **1** forms interactions of significant strength with *cis* dihydride complexes of platinum(II). The nature of this interaction is not affected by a change in the P−Pt−P bite angle, a somewhat surprising result. While intermolecular exchange can be stopped only at very low temperature for the dimethyl platinum derivative **9**, the solid-state structure of this adduct shows a rare agostic bonding mode for the bridging methyl groups. The methyl hydride derivative, **11**, undergoes slow exchange in solution at 25 °C and, in contrast to **9**, shows a Pt−C−Yb bonding mode in the solid state. The solution-state Yb−methyl interaction likely arises mainly as a result of the strong Yb−hydride interaction holding the Yb center near the methyl group (i.e., it results from conformational constraints) and appears to involve both Yb−C and C−H- -Yb interactions, although the exact nature of this interaction cannot be unequivocally determined from the solution-state data. An intermolecular exchange mechanism is introduced in the presence of excess platinum complex, for **5**, **7**, and **11**. Spin−spin communication between the two metal centers is present in **5**, **7**, and **11**. This communication is similar for **5** and **7** and roughly halved for **11**, but the precise mechanism(s) of this communication is (are) unknown.

We are continuing our investigations of the solution- and solid-state perturbations resulting from the interaction of **1** with various nonclassical Lewis bases. As above, the NMR-active ^{171}Yb isotope will be utilized in these studies. Our focus remains on stopped-exchange adducts, for which J_{YbX} values can be measured to give information concerning the nature of the Lewis acid−base interactions in the solution state. The results of these investigations will be reported at a later date.

Experimental Section

General Procedure. All reactions and product manipulations were carried out under dry nitrogen using standard Schlenk and drybox techniques. Solvents and reagents were dried and purified as described previously.[11] Infrared spectra, melting points, elemental analyses, and NMR spectra were obtained as previously described.[11]

^{1}H NMR shifts are relative to tetramethylsilane; the residual solvent peak was used as an internal reference. ^{31}P{^{1}H} NMR shifts are relative to 85% H_3PO_4 at δ 0.0, with shifts downfield of the reference considered positive. ^{195}Pt shifts are referenced to an absolute frequency scale relative to the proton signal of tetramethylsilane at 100.0000 MHz with Ξ defined to be exactly 21.4 MHz[60] and scaled according to the ^{1}H frequency of the particular machine used. A similar method was used for the ^{171}Yb referencing, with the standard being the reported frequency for $Cp^*_2Yb(thf)_2$[4b] and again scaled according to the ^{1}H frequency of the particular machine used. The HMQC or HSQC pulse sequence was used to acquire all of the 2-D spectra.[12,37] In all cases where metal

(60) Pregosin, P. S. In *Annual Reports on NMR Spectroscopy*; Webb, G. A., Ed.; Academic Press Inc.: London, 1986; Vol. 17.

chemical shifts were being investigated, first a large sweep width in the X dimension was used, and then the sweep width was narrowed, to assure that the resonances were not folded.

(dcype)Pt(μ-H)$_2$YbCp*$_2$ (5). To a solution of **4**[61] (0.15 g, 0.24 mmol) in toluene (10 mL) was added a solution of **1** (0.11 g, 0.25 mmol) in toluene (10 mL). The resulting dark blue solution was stirred at room temperature for 1 h and then filtered. Slow cooling of the filtrate to −40 °C gave **5** as dark maroon crystals. Concentration of the mother liquor, followed by cooling to −80 °C, gave a second crop of crystals, for a total yield of 0.19 g (75%), mp 308−310 °C (dec). The NMR data were measured on a sample made by adding C_6D_6 to a mixture of **1** (slight excess) and **4**. ^{1}H NMR (C_6D_6): δ 2.42 (s, 30H), 2.10−1.00 (m, 48H), −1.98 (m, 2H, $^1J_{PtH}$ = 1031 Hz, $^1J_{YbH}$ = 180 Hz, $^2J_{PH}$ = 152, 14 Hz) ppm. ^{31}P{^{1}H} NMR (C_6D_6): δ 75.4 (s, $^1J_{PtP}$ = 2077 Hz, J_{YbP} = 93 Hz). IR: 2718 w, 1889 s(br), 1416 w, 1379 m, 1345 w, 1293 m, 1271 m, 1195 w, 1173 m, 1119 m, 1109 s, 1043 m, 1004 s, 913 m, 888 m, 851 s, 822 m, 797 s, 751 s, 738 m, 724 w, 672 m, 650 m, 527 s, 510 w, 483 w, 393 w, 361 m cm^{-1}. Anal. Calcd for $C_{46}H_{80}P_2PtYb$: C, 52.0; H, 7.58. Found: C, 51.6; H, 7.28.

(dippe)Pt(CH_3)$_2$ (8). To a solution of dimethyl(1,5-cyclooctadiene)-platinum(II)[62] (0.33 g, 1.0 mmol) in CH_2Cl_2 (20 mL) was added dropwise a solution of dippe (0.26 g, 1.0 mmol) in CH_2Cl_2 (10 mL). The resulting light yellow solution was stirred at room temperature for 12 h. The solvent was removed under reduced pressure, the residue was dissolved in a 2:1 pentane:toluene solution (20 mL), and the resulting solution was filtered. Slow cooling of the filtrate to −40 °C yielded **8** as white crystals (0.38 g, 78%), mp 134−136 °C. ^{1}H NMR (C_6D_6): δ 2.05 (m, 4H), 1.23 (t, 6H, $^1J_{PtH}$ = 68 Hz, $^2J_{PH}$ = 7 Hz), 0.92 (m, 28H) ppm. ^{31}P{^{1}H} NMR (C_6D_6): δ 70.4 (s, $^1J_{PtP}$ = 1816 Hz). IR: 3594 s, 1409 w, 1379 s, 1362 s, 1297 w, 1252 m, 1239 s, 1193 m, 1176 m, 1161 m, 1106 m, 1091 m, 1079 m, 1028 s, 964 w, 926 m, 884 s, 861 m, 791 s, 695 s, 679 s, 651 s, 634 m, 617 s, 522 s, 509 s, 488 m, 467 m, 424 w, 386 m, 378 m, 278 m cm^{-1}. Anal. Calcd for $C_{16}H_{38}P_2Pt$: C, 39.4; H, 7.86. Found: C, 39.2; H, 7.59.

(dippe)Pt(μ-CH_3)$_2$YbCp*$_2$ (9). To a solution of **8** (0.43 g, 0.88 mmol) in toluene (20 mL) was added a solution of **1** (0.39 g, 0.88 mmol) in toluene (10 mL). Upon addition, the mixture immediately turned deep green and a green precipitate appeared. After being stirred at room temperature for 1 h, the mixture was warmed to 50 °C to dissolve all of the solid. The solution was filtered at 50 °C, and the filtrate was allowed to cool slowly to room temperature. Further slow cooling to −40 °C produced **9** as dark green crystals (0.70 g, 86%). Subsequent recrystallization from a 2:1 toluene:pentane solution (slow cooling to −40 °C) yielded X-ray quality crystals, mp 264−266 °C. ^{1}H NMR (C_6D_6): δ 2.28 (s, 30H), 1.92 (m, 4H, $-CH(CH_3)_2$), 0.85 (m, 28H), 0.68 (t, 6H, $^2J_{PtCH_3}$ = 66 Hz, $^3J_{PCH_3}$ = 7 Hz) ppm. ^{31}P{^{1}H} NMR (C_6D_6): δ 70.0 (s, $^1J_{PtP}$ = 1968 Hz). IR: 2725 m, 2285 w, 1382 s, 1366 m, 1296 w, 1285 w, 1253 m, 1239 w, 1172 w, 1161 w, 1134 w, 1105 w, 1091 w, 1080 w, 1029 s, 927 w, 884 m, 859 m, 797 m, 762 w, 725 w, 703 w, 684 s, 652 s, 620 m, 587 w, 520 m, 504 w, 490 m, 466 m, 425 w, 388 w, 369 m, 269 s cm^{-1}. Anal. Calcd for $C_{36}H_{68}P_2PtYb$: C, 46.4; H, 7.36. Found: C, 46.2; H, 7.42.

(dippe)Pt(CH_3)(OCOPh). To a Schlenk tube containing **8** (0.66 g, 1.4 mmol) and benzoic acid (0.33 g, 2.7 mmol) was added diethyl ether (40 mL). [It was found that using 1 equiv of benzoic acid results in only partial substitution, so that a mixture of **8** and the desired product was obtained.] The resulting pale yellow solution was stirred at room temperature for 60 h, during which time the crude product precipitated out of solution as a microcrystalline white solid. The solution was concentrated to 15 mL under reduced pressure, the solid was allowed to settle, and the solvent was removed *via* cannula. The white solid residue was washed with diethyl ether (2 × 15 mL, to remove the excess benzoic acid) and dissolved in toluene (20 mL), and the resulting solution was slowly cooled to −80 °C. Removal of the solvent from the crystals by cannula and drying under reduced pressure resulted in isolation of beige crystals. The mother liquor was concentrated and again cooled to −80 °C to yield a second crop of crystals. A third crop was obtained in a similar manner, giving a total yield of 0.41 g (51%), mp 148−155 °C. ^{1}H NMR (C_6D_6): δ 8.70 (m, 2H, meta-H), 7.21 (m, 3H, ortho/para-H), 2.20 (m, 2H, PC*H*$(CH_3)_2$), 1.81 (m, 2H, PC*H*$(CH_3)_2$), 1.27 (m, 6H), 0.92 (m, 24H) ppm. ^{31}P{^{1}H} NMR (C_6D_6): δ 74.5 (s, $^1J_{PtP}$ = 1843 Hz, *trans* to methyl), 70.1 (s, $^1J_{PtP}$ = 4025 Hz,*trans* to benzoate). IR: 1623 s (br), 1575 s, 1560 m, 1534 w, 1507 w, 1419 m, 1410 s, 1386 s, 1366 s, 1347 s, 1320 m, 1298 m, 1280 w, 1258 m, 1246 s, 1183 m, 1172 m, 1161 m, 1129 m, 1107 w, 1097 w, 1080 w, 1065 m, 1033 s, 1022 m, 994 w, 965 w, 940 m, 925 m, 884 s, 860 m, 831 m, 793 m, 719 s, 707 s, 690 s, 682 s, 669 s, 651 s, 644 m, 614 m, 580 w, 528 m, 489 m, 469 w, 456 m, 426 m cm^{-1}. Anal. Calcd for $C_{22}H_{40}P_2O_2Pt$: C, 44.5; H, 6.79. Found: C, 44.8; H, 6.82.

(dippe)Pt(CH_3)(H) (10). To a stirred thf solution (50 mL) of (dippe)Pt(CH_3)(OCOPh) (2.00 g, 3.40 mmol) was added dropwise a thf solution (50 mL) of $NaHB(OMe)_3$ (1.30 g, 10.2 mmol). A fine off-white precipitate immediately formed. The suspension was stirred for 12 h, the solvent was removed under reduced pressure, and the residue was extracted into toluene (2 × 15 mL). The solution was filtered, the filtrated was concentrated to 15 mL under reduced pressure, and then 50 mL of pentane was added. Slow cooling of the filtrate to −80 °C yielded crude **10** as a beige solid. Recrystallization from toluene:pentane (1:2) yielded pure **10** as a pale yellow solid (1.26 g, 79%), mp 63−66 °C. ^{1}H NMR (toluene-d_8): δ 2.04 (m, 4H), 1.82 (m, 4H), 1.44 (virtual t, 3H, $^2J_{PtCH_3}$ = 71 Hz), 1.08 (m, 12H), 0.82 (m, 12H), 0.48 (dd, 1H, $^1J_{PtH}$ = 1158 Hz, $^2J_{P\,trans\,H}$ = 201 Hz, $^2J_{P\,cis\,H}$ = 17.5 Hz) ppm. ^{31}P{^{1}H} NMR (toluene-d_8): δ 85.5 (s, $^1J_{PtP}$ = 1822 Hz, *trans* to methyl), 70.1 (s, $^1J_{PtP}$ = 1747 Hz, *trans* to hydride). IR: 1965 s(br), 1408 m, 1382 s, 1361 s, 1296 w, 1256 m, 1237 m, 1183 w, 1161 w, 1142 w, 1103 m, 1088 m, 1078 m, 1031 s, 930 m, 925 m, 885 s, 858 m, 805 m, 795 s, 768 m, 722 w, 697 s, 685 s, 670 s, 649 s, 639 s, 608 m cm^{-1}. Anal. Calcd for $C_{15}H_{36}P_2Pt$: C, 38.0; H, 7.66. Found: C, 38.3; H, 7.62.

(dippe)Pt(μ-CH_3)(μ-H)YbCp*$_2$ (11). To a toluene solution (15 mL) of **1** (0.18 g, 0.41 mmol) was added dropwise a toluene solution (15 mL) of **10** (0.18 g, 0.39 mmol). The resulting dark brown solution was filtered. Slow cooling of the filtrate to −40 °C yielded **11** as gold crystals. Concentration of the mother liquor followed by slow cooling to −80 °C gave a second crop of crystals, for a total yield of 0.26 g (70%), mp 220 °C (decomposition without melting). The NMR spectra were measured on a sample containing a slight excess of **1**. ^{1}H NMR (toluene-d_8): δ 2.29 (s, 30H), 1.85 (m, 4H), 1.1−0.85 (m, 16H), 0.80−0.60 (m, 15H), −2.65 (dd, 1H, $^1J_{PtH}$ = 1034 Hz, $^2J_{P\,trans\,H}$ = 163 Hz, $^2J_{P\,cis\,H}$ = 15 Hz, $^1J_{YbH}$ = 114 Hz) ppm. ^{31}P{^{1}H} NMR (toluene-d_8): δ 81.3 (s, $^1J_{PtP}$ = 1978 Hz, *trans* to methyl), 69.2 (s, $^1J_{PtP}$ = 2186 Hz, *trans* to hydride). IR: 2720 m, 1895 s(br), 1404 w, 1382 s, 1366 s, 1252 m, 1240 w, 1190 w, 1162 w, 1137 w, 1106 m, 1091 m, 1081 m, 1029 s, 965 w, 926 w, 885 m, 859 w, 797 m 706 m, 687 s, 654 s, 619 w cm^{-1}. Anal. Calcd for $C_{35}H_{66}P_2PtYb$: C, 45.8; H, 7.26. Found: C, 45.6; H, 7.25.

X-ray Crystal Structure Determinations of 9 and 11. (The X-ray details for **5** are available as supplementary material.) X-ray quality crystals of **9** were grown as described above. Dark green-brown blocks of **11** were grown by layering a pentane solution of **1** on top of a toluene solution of **10** and allowing the resulting solution to stand overnight at room temperature. Crystal data and numerical details of the structure determinations for **9** and **11** are given in Tables 4, 5, 8, and 9. The crystals were placed in Paratone N oil, mounted on the end of a cut quartz capillary tube, and placed under a flow of cold nitrogen on an Enraf-Nonius CAD4 diffractometer. Intensities were collected with graphite-monochromatized Mo Kα (λ = 0.710 73 Å) radiation using the θ−2θ scan technique. Lattice parameters were determined using automatic peak search and indexing procedures. Intensity standards were measured every hour of data collection.

The raw intensity data were converted to structure factor amplitudes and their esd's by correction for scan speed, background, and Lorentz and polarization effects. Corrections for crystal decomposition were performed on the data obtained on **9**, but no correction was necessary for the data obtained for **11**. A θ-independent absorption correction using the program DIFABS[30] was applied to the data for **9** and **11**, using the isotropic models as a basis for the correction. The structure of **9** was solved by Patterson techniques, while that of **11** was solved

(61) *cis*-(dcype)PtH_2 (**4**) and *cis*-(dcypp)PtH_2 (**6**) were prepared *via* the procedure described in ref 8; the spectroscopic properties of both complexes were identical to those reported in ref 17.

(62) Clark, H. C.; Manzer, L. E. *J. Organomet. Chem.* **1973**, *59*, 411.

using SHELXS-86,[63] and refined using standard least-squares and Fourier techniques.

The data for **9** at this point (anisotropic model) indicated that placement of the hydrogens based on idealized bonding geometry was justified. These atoms were placed in the idealized positions and included in the structure factor calculation but not refined (all hydrogen atoms were given isotropic thermal parameters $1.2(B_{iso})$ of the carbon to which they were attached). Examination of a difference Fourier map showed five positive peaks of intensity 0.48−0.83 e Å^{-3} *ca.* 1.0 Å from the two bridging methyl carbons, oriented roughly tetrahedrally around the carbons. These peaks were assigned as the hydrogen atoms of C1 and C2, with the sixth hydrogen (H2C) added on the basis of idealized bonding geometry. These atoms were treated in a manner similar to that of the other hydrogen atoms, above.

The Fourier difference map of the isotropic model for **11**, after the absorption correction, revealed several cases of disorder which were modeled as follows: one Cp* ring consists of six carbon atoms, two of which were assigned a multiplicity of 0.5; the other Cp* ring also consists of six carbon atoms, with three adjacent atoms assigned a multiplicity of 0.67; there are 10 methyl carbon atoms on each Cp* ring, each of multiplicity 0.5 (a result of two major orientations of the ring, about the ring centroid axis); the $(CH_2)_2$ bridge of the phosphine was modeled as four carbon atoms, each of multiplicity 0.5 (arising from the two possible geometries of this bridge); two of the isopropyl groups of the phosphine were found to be rotationally disordered about the ipso carbon atom, and these were modeled by adding a third methyl carbon and assigning two of the methyl carbons a multiplicity of 0.5 (the third methyl kept at multiplicity 1.0); another of the isopropyl groups of the phosphine was found to be disordered about the P−C_{ipso} bond (a result of two different orientations of this group), and two separate isopropyl groups were used to model this disorder, one of the isopropyl groups assigned a muliplicity of 0.67 and the other a multiplicity of 0.33.

A θ-independent DIFABS absorption correction was then applied to the raw data, using this improved model as a basis. The model was then refined isotropically and then anisotropically (only the heavy atoms, and the carbon atoms of multiplicity 1.0 (14 of the 35 total carbon atoms) were refined anisotropically). At this point, 16 reflections were rejected on the basis of large $w(\Delta^2)$ values, as well as a trend in *hkl*: they were all of the form *h*, 0, 0; 2*h*, *h*, 0; 3*h*, *h*, 0; etc.; or very nearly so. Analysis of the difference map at this point indicated that inclusion of the hydrogen atoms at idealized locations was not justified by the quality of the data, and so no hydrogens were included in the model. No difference peaks near the bridging methyl carbon or near the expected hydride location were present. The most intense difference peak, 6.6 e Å^{-3}, was located near the Pt center. The next most intense peak was 2.3 e Å^{-3}; the top seven most intense peaks (seventh peak = 1.2 e Å^{-3}) were associated with the Pt and Yb centers.

The least-squares program minimized the expression, $\sum w(|F_o| - |F_c|)^2$, where w is the weight of a given observation. Values of 0.03 (**9**) and 0.05 (**11**) for the p factor were used to reduce the weight of intense reflections in the refinements. The analytical forms of the scattering factor tables for the neutral atoms were used, and all non-hydrogen scattering factors were corrected for both real and imaginary components of anomalous dispersion.

Acknowledgment. This work was supported by the Director, Office of Energy Research, Office of Basic Energy Sciences, Chemical Sciences Division of the U.S. Department of Energy under Contract No. DE-AC03−76F00098. We thank the National Science Foundation for a predoctoral fellowship to D.J.S. and Dr. F. J. Hollander for helpful advice concerning X-ray crystallography.

Supplementary Material Available: Crystallographic summary, data, and positional parameters for **5**, complete tables of bond lengths and angles, anisotropic thermal parameters, and root mean square amplitudes of thermal vibration for **9** and **11**, NMR spectra for **7** and **11**, and an ORTEP diagram of the structure of **11** showing all atoms (59 pages); observed and calculated structure factors for **9** and **11** (65 pages). The following NMR spectra are included: $^1H/^{195}Pt$ and $^1H/^{171}Yb$ HMQC spectra of **7** (300 MHz, 25 °C, C_6D_6); $^1H/^{195}Pt$ HMQC spectrum of **11** (300 MHz, −70 °C, toluene-d_8); $^1H/^{31}P$ HMQC spectrum of **11** (300 MHz, −70 °C, toluene-d_8), showing J_{YbP} for the phosphorus nucleus *trans* to the methyl group. This material is contained in many libraries on microfiche, immediately follows this article in the microfilm version of the journal, can be ordered from the ACS, and can be downloaded from the Internet; see any current masthead page for ordering information and Internet access instructions.

JA943952B

(63) Sheldrick, G. M. *Acta Crystallogr.* **1990**, *A46*, 467.